Published OnlineFirst July 19, 2012; DOI:10.1158/0008-5472.CAN-12-0943



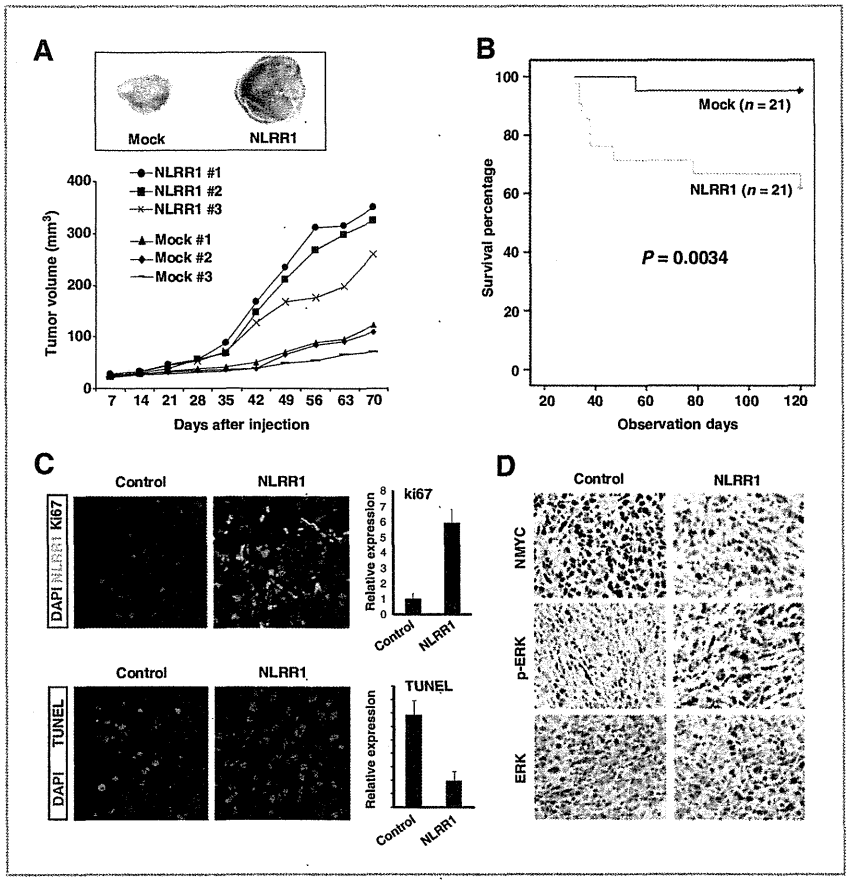


Figure 6. Neuroblastoma cells stably expressing NLRR1 accelerate tumor growth in nude mice. A, after subcutaneous injection of mock- and NLRR1-stably expressing SH-SY5Y clones into nude mice, tumor volumes were measured on the indicated days. The data represent the mean value. Top panel shows representative pictures of tumors 70 days after injection. B, Kaplan–Meyer survival curve of mice-bearing mock- and NLRR1-stably expressing SH-SY5Y xenografts. C, detection of NLRR1 and Ki-67 expression in the mock- and NLRR1-expressing tumor xenografts (top). TUNEL staining shows that NLRR1 tumor has reduced apoptotic cells (bottom). D, IHC data show the staining image of NMYC, p-ERK, and ERK in NLRR1 versus control tumors.

## Discussion

Upregulated MKK-ERK signaling is known to be involved in the genesis of several cancers (18–21). Multidrug-resistant human neuroblastoma cells have three- to 30-fold more cell surface EGFRs than the drug-sensitive parental cells (36), indicating that EGFRs may play an important role in the aggressiveness of human neuroblastoma. EGF stimuli activated MAPK in neuroblastoma (16) and IGF-1 enhanced neuroblastoma cell proliferation via activation of MAPK (17). NLRR family proteins are considered to modulate cellular signaling, especially that of MAPKs (15). Although it was reported that overexpression of NLRR1 enhances cell proliferation and inhibits cellular apoptosis in neuroblastoma, our previous study did not rule out the involvement of NLRR1 with EGF and IGF-1 signaling. Here, we first report that ectopic expression of NLRR1 also enhanced EGF- and IGF-1–mediated cellular proliferation, which is inhibited in cells treated with MEK1/2 inhibitor. This suggests that NLRR1-mediated promotion of proliferation is at least in part dependent on activation of ERK. However, the method by which NLRR1 enhances EGFR and IGFR signaling still needs to be clarified. Another NLRR family protein, NLRR3, was reported to induce phosphorylation of ERK in response to EGF (15), suggesting the possibility that NLRR1 that is 54% homology to NLRR3 may also induce ERK phosphorylation. Our results propose that NLRR1 is important in enhancing ERK phosphorylation in cells upon EGF and IGF stimuli. Interestingly, NLRR1 affects p-ERK and p-AKT in different extent (Fig. 2B) that depends on cell lines (data not shown). The reason behind this selectivity is unknown and need to be addressed further in the future.

ERK is known to phosphorylate many transcriptional factors, including Sp1 (33, 37). Moreover, Sp1 and E2F1 are reported to transcriptionally regulate *MYCN* in neuroblastoma (31, 32). Therefore, there may be an important link between the activation of ERK and *MYCN* induction, which is further supported by the evidence that IGF-1 can induce *MYCN* via activation of MAPK (17). However, in this report of EGF-1-mediated MYCN induction, the involvement of Sp1 or E2F1 was not explained. Here, we report that EGF induces *MYCN* via the EGFR-ERK pathway. Several stimuli, including retinoic acid and TGF-β repress the *MYCN* gene, and are associated with recruited Sp1 and E2F1 and their other cofactors (31, 38). By using ChIP assays, we observed that Sp1 but not E2F1 was recruited to the *MYCN* promoter in response to EGF. However, it has been reported that the presence of Sp1 is not always sufficient to activate a transcriptionally silent *MYCN* gene (32).

Published OnlineFirst July 19, 2012; DOI:10.1158/0008-5472.CAN-12-0943



Therefore, we have further investigated whether Sp1 is important for *MYCN* induction in our experimental conditions. siRNA-mediated knockdown of *Sp1*-reduced *MYCN* expression and also inhibited cell proliferation, suggesting that Sp1-mediated *MYCN* induction regulates cell proliferation. Using luciferase reporter assays, we identified the responsive Sp1-binding element in the promoter region for *MYCN* induction. Sp1 phosphorylation is a prerequisite for the interaction with genomic DNA (33). Therefore, we also investigated whether EGF induces Sp1 phosphorylation and enhances its recruitment to the *MYCN* promoter. Western blotting data showed that EGF treatment enhanced phosphorylation of Sp1, and the MEK1/2 inhibitor U0126 inhibited this phosphorylation event, supporting the previous report that ERK induces Sp1 phosphorylation (33). Using the dephosphorylating agent CIAP, we further confirmed that phospho-Sp1 is involved in the transactivation of *MYCN* by recruitment to the genomic DNA of the *MYCN* promoter. Collectively, this evidence suggests that EGF induces *MYCN* through phospho-Sp1 recruitment to the *MYCN* promoter. However, MYCN induction by IGF-1 was not investigated in the present study, but we speculate that it may be by the same mechanism as EGF, because IGF-1 has been reported to activate MAPK in neuroblastoma.

Another new finding of our current study is that *MYCN* is induced after ectopic expression of *NLRR1* in neuroblastoma cells. Under our experimental conditions, EGF-mediated *MYCN* induction was accelerated in *NLRR1*-overexpressing cells and inhibited in *NLRR1*-knockdown cells, suggesting that NLRR1 enhances *MYCN* induction and activation of ERK. In addition, NLRR1 overexpression enhanced Sp1 recruitment to the *MYCN* promoter. We previously reported that *NLRR1* transcriptionally regulated by MYCN is highly expressed in aggressive neuroblastoma (14). *NLRR1* was also found to be highly expressed in *MYCN*-amplified tumors compared with that of *MYCN* nonamplified neuroblastoma. Therefore, we suggest that MYCN directly regulates NLRR1, and that NLRR1 further induces *MYCN* through the activation of the EGFR-ERK cascade, suggesting a positive feedback loop between NLRR1 and MYCN that may lead to aggressive neuroblastoma. To this notion, we further determined the *in vivo* tumorigenic activity of NLRR1 in *MYCN* nonamplified SH-SY5Y cells, which are well known to form tumors in nude mice (39, 40). Our results show that SH-SY5Y cells stably expressing NLRR1 rapidly proliferate in culture medium and in nude mice, and promote decreased survival rates among inoculated mice, presumably by induced endogenous *MYCN*.

In conclusion, our results provide significant evidence that that NLRR1 enhances ERK signaling to induce *MYCN*, which may play major roles in the progression of aggressive neuroblastoma. Taking note that *MYCN* highly expressing tumors are often resistant to antitumor therapies, new drug discovery blocking NLRR1-mediated ERK signaling to control *MYCN* expression may be an attractive choice in treating aggressive neuroblastoma.

## Disclosure of Potential Conflicts of Interest

No potential conflicts of interest were disclosed.

## Authors' Contributions

**Conception and design:** S. Hossain, A. Takatori, A. Nakagawara
**Development of methodology:** S. Hossain, A. Takatori, Y. Suenaga, T. Kamijo
**Acquisition of data (provided animals, acquired and managed patients, provided facilities, etc.):** S. Hossain, A. Takatori, Y. Nakamura
**Analysis and interpretation of data (e.g., statistical analysis, biostatistics, computational analysis):** S. Hossain, A. Takatori
**Writing, review, and/or revision of the manuscript:** S. Hossain, A. Nakagawara
**Administrative, technical, or material support (i.e., reporting or organizing data, constructing databases):** Y. Suenaga, Y. Nakamura, T. Kamijo, A. Nakagawara
**Study supervision:** A. Nakagawara

## Acknowledgments

We thank Drs. M. Ohira, T. Ozaki, J. Akter, and K. Hasan (Chiba Cancer Center Research Institute, Chiba, Japan) for the fruitful discussion and assistance.

## Grant Support

This work was supported by a Grant-in-Aid from the Ministry of Health, Labour, and Welfare for Third Term Comprehensive Control Research for Cancer (A. Nakagawara), a Grant-in-Aid for Scientific Research on Priority Areas from the Ministry of Education, Culture, Sports, Science, and Technology, Japan (A. Nakagawara), a grant from the Takeda Science Foundation, and a Grant-in-Aid for Scientific Research from the Japanese Society for the Promotion of Science (A. Takatori and A. Nakagawara).

The costs of publication of this article were defrayed in part by the payment of page charges. This article must therefore be hereby marked *advertisement* in accordance with 18 U.S.C. Section 1734 solely to indicate this fact.

Received March 16, 2012; revised May 21, 2012; accepted June 6, 2012; published OnlineFirst July 19, 2012.

## References

1. Brodeur GM. Neuroblastoma: biological insights into a clinical enigma. Nat Rev Cancer 2003;3:203–16.
2. Weinstei JL, Katzenstein HM, Cohn SL. Advances in the diagnosis and treatment of neuroblastoma. Oncologist 2003;8:278–92.
3. Brodeur GM, Nakagawara A. Molecular basis of clinical heterogeneity in neuroblastoma. Am J Pediatr Hematol Oncol 1992;14:111–6.
4. Bown N, Cotterill S, Lastowska M, O'Neill S, Pearson AD, Plantaz D, et al. Gain of chromosome arm 17q and adverse outcome in patients with neuroblastoma. N Engl J Med 1999;340:1954–61.
5. Frappaz D, Michon J, Coze C, Berger C, Plouvier E, Lasset C, et al. LMCE3 treatment strategy: results in 99 consecutively diagnosed stage 4 neuroblastomas in children older than 1 year at diagnosis. J Clin Oncol 2000;18:468–76.
6. Schmidt ML, Lukens JN, Seeger RC, Brodeur GM, Shimada H, Gerbing RB, et al. Biologic factors determine prognosis in infants with stage IV neuroblastoma: a prospective Children's Cancer Group study. J Clin Oncol 2000;18:1260–8
7. Felsher DW, Bishop JM. Reversible tumorigenesis by MYC in hematopoietic lineages. Mol Cell 1999;4:199–207.
8. D'Cruz CM, Gunther EJ, Boxer RB, Hartman JL, Sintasath L, Moody SE, et al. c-MYC induces mammary tumorigenesis by means of a preferred pathway involving spontaneous Kras2 mutations. Nat Med 2001;7:235–9.
9. Pelengaris S, Littlewood T, Khan M, Elia G, Evan G. Reversible activation of c-Myc in skin: induction of a complex neoplastic phenotype by a single oncogenic lesion. Mol Cell 1999;3:565–77.
10. Taguchi A, Wanaka A, Mori T, Matsumoto K, Imai Y, Takagi T, et al. Molecular cloning of novel leucine-rich repeat proteins and their expression in the developing mouse nervous system. Brain Res Mol Brain Res 1996;35:31–40.

Published OnlineFirst July 19, 2012; DOI:10.1158/0008-5472.CAN-12-0943




11. Taniguchi H, Tohyama A, Takagi T. Cloning and expression of a novel gene for a protein with leucine-rich repeats in the developing mouse nervous system. Brain Res Mol Brain Res 1996;36:45–52.
12. Hamano S, Ohira M, Isogai E, Nakada K, Nakagawara A. Identification of novel human neuronal leucine-rich repeat (hNLRR) family genes and inverse association of expression of Nbla10449/hNLRR-1 and Nbla1067/hNLRR-3 with the prognosis of primary neuroblsatoma. Int J Oncol 2004;24:1457–66.
13. Bando T, Sekine K, Kobayashi S, Watabe AM, Rump A, Tanaka M, et al. Neuronal leucine-rich repeat protein 4 functions in hippocampus-dependent long-lasting memory. Mol Cell Biol 2005;25:4166–75.
14. Hossain MS, Ozaki T, Wang H, Nakagawa A, Takenobu H, Ohira M, et al. N-MYC promotes cell proliferation through a direct transactivation of neuronal leucine-rich repeat protein-1 (NLRR1) gene in neuroblastoma. Oncogene 2008;27:6075–82.
15. Fukamachi K, Matsuoka Y, Ohno H, Hamaguchi T, Tsuda H. Neuronal leucine-rich repeat protein-3 amplifies MAPK activation by epidermal growth factor through a carboxy-terminal region containing endocytosis motifs. J Biol Chem 2002;277:43549–52.
16. Ho R, Mintum JE, Hishiki T, Zhao H, Wang Q, Cnaan A, et al. Proliferation of human neuroblastomas mediated by the epidermal growth factor receptor. Cancer Res 2005;65:9868–75.
17. Misawa A, Hosoi H, Arimoto A, Shikata T, Akioka S, Matsumura T, et al. N-Myc induction stimulated by insulin-like growth factor I through mitogen-activated protein kinase signaling pathway in human neuroblastoma cells. Cancer Res 2000;60:64–9.
18. Chang L, Karin M. Mammalian MAP kinase signalling cascades. Nature 2001;410:37–40.
19. Johnson GL, Lapadat R. Mitogen-activated protein kinase pathways mediated by ERK, JNK, and p38 protein kinases. Science 2002;298: 1911–2.
20. Dunn KL, Espino PS, Drobic B, He S, Davie JR. The Ras-MAPK signal transduction pathway, cancer and chromatin remodeling. Biochem Cell Biol 2005;83:1–14.
21. Davies H, Bignell GR, Cox C, Stephens P, Edkins S, Clegg S, et al. Mutations of the BRAF gene in human cancer. Nature 2002;417: 949–54.
22. Jeffers M, Fiscella M, Webb CP, Anver M, Koochekpour S, Vande Woude GF. The mutationally activated Met receptor mediates motility and metastasis. Proc Natl Acad Sci U S A 1998;95:14417–22.
23. Webb CP, Taylor GA, Jeffers M, Fiscella M, Oskarsson M, Resau JH, et al. Evidence for a role of Met-HGF/SF during Ras-mediated tumorigenesis/metastasis. Oncogene 1998;17:2019–25.
24. Ward Y, Wang W, Woodhouse E, Linnoila I, Liotta L, Kelly K. Signal pathways which promote invasion and metastasis: critical and distinct contributions of extracellular signal-regulated kinase and Ral-specific guanine exchange factor pathways. Mol Cell Biol 2001;21: 5958–69.
25. Ghos AK, Steele R, Ray RB. Carboxy-terminal repressor domain of MBP-1 is sufficient for regression of prostate tumor growth in nude mice. Cancer Res 2005;65:718–21.
26. Konstantinidou G, Bey EA, Rabellino A, Schuster K, Maira MS, Gazdar AF, et al. Dual phosphoinositide 3-kinase/mammalian target of rapamycin blockade in an effective radiosensitizing strategy for the treatment of non-small cell lung cancer harboring K-ras mutations. Cancer Res 2009;69:7644–52.
27. Wang J, Zhou J, Wu GS. ERK-dependent MKP-1-mediated cisplatin resistance in human ovarian cancer cells. Cancer Res 2007;67: 11933–41.
28. Maity A, Pore N, Lee J, Solomon D, O'Rourke DM. Epidermal growth factor receptor transcriptionally up-regulates vascular endothelial growth factor expression in human glioblastoma cells via a pathway involving phosphatidylinositol 3′-kinase and distinct from that induced by hypoxia. Cancer Res 2000;60:5879–86.
29. Davisll JW, Lauer FT, Burdick AD, Hudson LG, Burchiel SW. Prevention of apoptosis by 2,3,7,8-Tetrachlorodibenzo-p-dioxin (TCDD) in the MCF-10A cell line: correlation with increased transforming growth factor $\alpha$ production. Cancer Res 2001;61:3314–20.
30. Zhou Y, Brattain MG. Synergy of epidermal growth factor receptor kinase inhibitor AG1478 and ErbB2 kinase inhibitor AG879 in human colon carcinoma cells is associated with induction of apoptosis. Cancer Res 2005;65:5848–56.
31. Strieder V, Lutz W. E2F proteins regulate MYCN expression in neuroblastomas. J Biol Chem 2003;278:2983–9.
32. Kramps C, Strieder V, Sapetschnig A, Suske G, Lutz W. E2F and Sp1/Sp3 Synergize but are not sufficient to activate the MYCN gene in neuroblastomas. J Biol Chem 2004;279:5110–7.
33. Merchant JL, Du M, Todisco A. Sp1 phosphorylation by Erk 2 stimulates DNA binding. Biochem Biophys Res Commun 1999; 254:454–61.
34. Jia Z, Zhang J, Wei D, Wang L, Yuan P, Le X, et al. Molecular basis of the synergestic sntiangiogenesis activity of Bevacizumab and Mithramycin A. Cancer Res 2007;67:4878–85.
35. Matsuoka T, Zhao L, Stein R. The DNA binding activity of the RIPE3b1 transcription factor of insulin appears to be influenced by tyrosine phosphorylation. I Biol Chem 2001;276:22071–6.
36. Meyers MB, Shen WP, Spengler BA, Ciccarone V, O'Brien JP, Donner DB, et al. Increased epidermal growth factor receptor in multidrug-resistant human neuroblastoma cells. J Cell Biochem 1988;38:87–97.
37. Milanini-Mongiat J, Pouyssegur J, Pages G. Identification of two Sp1 phohphorylation sites for p42/44 mitogen-activated protein kinases. J Bio Chem 2002;277:20631–9.
38. Ferreira R, Naguibneva I, Pritchard LL, Ait-Si-Ali S, Harel-Bellan A. The Rb/chromatin connection and epigenetic control: opinion. Oncogene 2001;20:3128–33.
39. Aoyama M, Ozaki T, Inzuka H, Tomotsune D, Hirato J, Okamoto Y, et al. LMO3 interacts with neuronal transcription factor, HEN2, and acts as an oncogene in neuroblastoma. Cancer Res 2005:65:4587–97.
40. Eggert A, Grotzer MA, Ikegaki N, Liu XG, Evans AE, Brodeur GM. Expression of the neurotrophin receptor TrkA down-regulates expression and fuinction of angiogenic stimulators in SH-SY5Y neuroblastoma cells. Cancer Res 2002;62:1802–8.

Development 138, 1471-1482 (2011) doi:10.1242/dev.053652


# Polycomblike 2 facilitates the recruitment of PRC2 Polycomb group complexes to the inactive X chromosome and to target loci in embryonic stem cells

**Miguel Casanova[1,*], Tanja Preissner[1,*], Andrea Cerase[1], Raymond Poot[2], Daisuke Yamada[3], Xiangzhi Li[3], Ruth Appanah[1], Karel Bezstarosti[4], Jeroen Demmers[4], Haruhiko Koseki[3] and Neil Brockdorff[1,†]**

## SUMMARY

Polycomb group (PcG) proteins play an important role in the control of developmental gene expression in higher organisms. In mammalian systems, PcG proteins participate in the control of pluripotency, cell fate, cell cycle regulation, X chromosome inactivation and parental imprinting. In this study we have analysed the function of the mouse PcG protein polycomblike 2 (Pcl2), one of three homologues of the *Drosophila* Polycomblike (Pcl) protein. We show that Pcl2 is expressed at high levels during early embryogenesis and in embryonic stem (ES) cells. At the biochemical level, Pcl2 interacts with core components of the histone H3K27 methyltransferase complex Polycomb repressive complex 2 (PRC2), to form a distinct substoichiometric biochemical complex, Pcl2-PRC2. Functional analysis using RNAi knockdown demonstrates that Pcl2-PRC2 facilitates both PRC2 recruitment to the inactive X chromosome in differentiating XX ES cells and PRC2 recruitment to target genes in undifferentiated ES cells. The role of Pcl2 in PRC2 targeting in ES cells is critically dependent on a conserved PHD finger domain, suggesting that Pcl2 might function through the recognition of a specific chromatin configuration.

**KEY WORDS: ES cell, Polycomb, X inactivation, Mouse**

## INTRODUCTION

In higher organisms the execution and maintenance of cell fate decisions in early development depend critically on epigenetic mechanisms that confer heritable on/off states at specific target loci. The Polycomb group (PcG) proteins play a central role in this, establishing and maintaining gene repression at target loci predominantly via post-translational modification of the core histones. Initially identified as mediators of cellular memory at *Hox* loci in *Drosophila* (Lewis, 1978), PcG proteins have been found to be highly conserved and to contribute to developmental gene regulation, the cell cycle, the maintenance of pluripotency and self-renewal capability in embryonic and adult stem cells and to epigenetic silencing on the inactive X chromosome (Xi) and at parentally imprinted loci (for reviews, see Sparmann and van Lohuizen, 2006; Schuettengruber and Cavalli, 2009; Simon and Kingston, 2009).

There are two major multimeric PcG protein complexes that have been widely studied: Polycomb repressive complex (PRC) 1 and 2. The PRC2 complex catalyses histone H3K27 methylation (Cao et al., 2002; Czermin et al., 2002; Muller et al., 2002; Kuzmichev et al., 2002) and is generally thought to be early acting, providing a binding site for subsequent recruitment of PRC1. PRC1 functions as an E3 ligase that specifically monoubiquitylates histone H2A (de Napoles et al., 2004; Wang, H. et al., 2004; Cao et al., 2005; Elderkin et al., 2007). H2A ubiquitylation is important for PcG-mediated silencing (Stock et al., 2007; Nakagawa et al., 2008), although there is also evidence that other direct and/or indirect mechanisms contribute to PRC1 function (Francis et al., 2001; Gambetta et al., 2009).

Mechanisms involved in the targeting of PcG complexes to specific loci remain poorly understood. In *Drosophila*, the recruitment to Hox genes and probably other target loci is mediated by cis-acting regions that are essential for silencing: the Polycomb response elements (PREs) (Simon et al., 1993; Chan et al., 1994). PREs have not been well defined in mammalian cells, although a recent report described a single example associated with the *MafB* locus (Sing et al., 2009). In the case of X inactivation, recruitment of PcG proteins is dependent upon the expression of non-coding RNAs (Plath et al., 2003; Silva et al., 2003; de Napoles et al., 2004; Kohlmaier et al., 2004; Plath et al., 2004), and this might also be the case at some imprinted loci (Umlauf et al., 2004; Nagano et al., 2008).

The PRC2 complex comprises three unique core protein components – the histone methyltransferase Ezh2, Eed and Suz12 – and the generic histone-binding proteins RbAp46/48 (also known as Rbbp7/4) (Cao et al., 2002; Czermin et al., 2002; Muller et al., 2002; Kuzmichev et al., 2002). The core PRC2 proteins do not bind DNA, suggesting that co-factors might be important in targeting the complex to specific loci. In this regard, candidate proteins associated with PRC2 have been identified in genetic and biochemical screens. The Jarid2 protein was recently shown to interact with PRC2 in mouse embryonic stem (ES) cells and has been suggested to play a role in PRC2 targeting (Peng et al., 2009; Shen et al., 2009; Li et al., 2010; Pasini et al., 2010) and/or in establishing the poised state at PcG target loci (Landeira et al., 2010). AEBP2, a zinc-finger protein, co-purifies with PRC2 in Hela cells (Pasini et al., 2010) and ES cells (Peng et al., 2009;

[1]Developmental Epigenetics Group, Department of Biochemistry, University of Oxford, South Parks Road, Oxford OX1 3QU, UK. [2]Department of Cell Biology, Erasmus Medical Centre, Dr Molewaterplein 50, 3015GE Rotterdam, The Netherlands. [3]RIKEN Research Center for Allergy and Immunology, JST, CREST, 1-7-22 Suehiro, Tsurumi-ku, Yokohama 230-0045, Japan. [4]Proteomics Centre, Erasmus Medical Centre, Dr Molewaterplein 50, 3015GE Rotterdam, The Netherlands.

*These authors contributed equally to this work
†Author for correspondence (neil.brockdorff@bioch.ox.ac.uk)

**Accepted 17 January 2011**

Shen et al., 2009; Li et al., 2010; Landeira et al., 2010) but its function is as yet undetermined. Finally, the Polycomblike (Pcl) protein associates with PRC2 in *Drosophila* (O'Connell et al., 2001; Tie et al., 2003; Papp and Muller, 2006) and in mammalian cells (Cao et al., 2008; Sarma et al., 2008) and has been proposed to have a role in stimulating H3K27me3 activity and/or targeting of the complex (Nekrasov et al., 2007; Cao et al., 2008; Sarma et al., 2008).

In this study we have analysed the function of the mouse Pcl2 (Mtf2 – Mouse Genome Informatics) protein, one of three homologues of Pcl found in mammalian cells. We find that Pcl2 is expressed at high levels during early embryogenesis and in ES cells. Pcl2 interacts with the core PRC2 complex to form a stable and distinct biochemical complex, Pcl2-PRC2. Functional analysis using RNAi knockdown demonstrates that Pcl2-PRC2 is important in PRC2 recruitment to the Xi in differentiating XX ES cells and also for PRC2 recruitment to target genes in undifferentiated ES cells. A conserved PHD finger domain in Pcl2 is required for PRC2 targeting in ES cells.

## MATERIALS AND METHODS

### Cell lines and embryos

Growth and maintenance of trophoblast stem (TS) and ES cell lines were as described previously (Penny et al., 1996; Mak et al., 2002). ES cell differentiation was achieved by embryoid body formation via removal of LIF from the medium. The MP fibroblast cell line was derived in house from a male PGK mouse.

Preimplantation and postimplantation mouse embryos were obtained from timed mating of C57B16×CBA F1 animals as described previously (Sheardown et al., 1997).

### Immunofluorescence (IF) and RNA fluorescent in situ hybridisation (FISH) analyses

Preparation of cells and of embryos for IF, RNA FISH and Immuno-RNA FISH were as previously described (Sheardown et al., 1997; Mak et al., 2002; Silva et al., 2003; de Napoles et al., 2004). IF, RNA FISH and Immuno-RNA FISH were carried out as described previously (Mak et al., 2002; Silva et al., 2003; de Napoles et al., 2004). When using Pcl2 antibody for IF, cells were pre-extracted prior to fixation by treatment with 0.4% Triton X-100 (1 minute, 4°C). Primary antibodies were diluted in 5% normal goat serum in 0.2% fish gelatin: H3K27me3, Ezh2 and Suz12 (all Millipore) 1:500; Eed (Sewalt et al., 1998) 1:100. Pcl2 mouse monoclonal antibody was from H.K. and is described in a separate publication (Li et al., 2011). Pcl2 antibody incubation was carried out in CanGetSignal solution (Toyobo, Japan; 1:10). Images were acquired on a Leica DMRB fluorescence microscope using a CCD camera or, alternatively, on a Leica TCS SP5 confocal microscope using LAS AF software. For Immuno-RNA-FISH of ES cell colonies, images were acquired on a Deltavision real-time (RT) microscope (Applied Precision; 63× objective with a numerical aperture of 1.4). Images were deconvolved with Softworx, and ImageJ was used for further image processing. Maximum intensity projections are shown.

### Generation of stable Pcl2-FLAG cell lines

*Pcl2* full-length cDNA was amplified from PGK12.1 ES cell mRNA using oligonucleotides 5′-GGATCCACCATGAGAGACTCTACAGGAGCA-3′ and 5′-GGTACCACCTCCGGATGCAGTCGCTCCTTCCCA-3′. cDNA was cloned N-terminally to the FLAG tag into the 5′ *Bam*HI and 3′ *Kpn*I sites of the pCBA-2×FLAG vector (van den Berg et al., 2008). pCBA-Pcl2-2×FLAG construct was transfected into PGK12.1 ES cells using Lipofectamine 2000 (Invitrogen) according to the manufacturer's instructions and stable transformants were selected with geneticin (400 μg/ml, Gibco) for 10 days. Individual colonies were picked, expanded and analysed by western blotting for stable expression of Pcl2-2×FLAG.

Pcl2 deletion constructs were generated by 'PCR sewing' using the above construct as a template and the oligonucleotides listed in Table S2 in the supplementary material to induce deletion of specific domains by fusion of two regions of the cDNA. Cloning of PCR products in pCBA-2×FLAG, transfection and clone selection were as described above.

### Generation of stable Pcl2 knockdown cell lines

For each short hairpin RNA (shRNA) construct, four complementary oligonucleotides with overhangs and loop sequence were synthesised, annealed and cloned into the *Bgl*II/*Hin*dIII sites of the pSuper.neo/gfp vector (OligoEngine). Hairpin constructs were transfected into PGK12.1 ES cells using Lipofectamine 2000. Stable transformants were selected with geneticin (400 μg/ml) for 4 days and by FACS sorting for GFP expression. Sorted cells were plated at clonal density and individual colonies were picked, expanded and Pcl2 levels were analysed by western blotting. shRNA target sequences are listed in Table S3 in the supplementary material.

### Cell fractionation and western blot analysis

The preparation of nuclear extracts and cell fractionation were essentially as described previously (Elderkin et al., 2007; van den Berg et al., 2010). For western blotting, proteins were separated on SDS-PAGE gels and transferred (45 minutes, 15V) to PVDF membranes in 1× Transfer buffer (48 mM Tris, 39 mM glycine, 0.037% SDS, 20% methanol) using a Bio-Rad semi-dry blotting system. Enhanced chemiluminescence detection was performed as recommended by the manufacturer (GE Healthcare). The following antibodies and dilutions were used for western blotting: Eed mouse monoclonal (Sewalt et al., 1998), 1:200; Ezh2 rabbit polyclonal (Millipore), 1:1000; Suz12 rabbit polyclonal (Millipore), 1:1000; M2 FLAG (Sigma), 1:2000; Ring1B (Rnf2 – Mouse Genome Informatics) mouse monoclonal (de Napoles et al., 2004), 1:100; YY1 rabbit polyclonal (Santa Cruz), 1:200; HP1γ (Millipore), 1:1000; Rbpj (Millipore), 1:1000; lamin B goat polyclonal (Santa Cruz), 1:2000; H3K27me3 (Millipore), 1:1000; H2A, H4, H3K4me1, H3K4me3 (Millipore), 1:2000; and H3, H3K4me2, H3K27me1, H3K27me2 rabbit polyclonal (Millipore), 1:5000. To improve detection, Pcl2 antibody was diluted (1:100) in CanGetSignal solution according to the manufacturer's instructions. Acid-extracted histones were prepared as described previously (de Napoles et al., 2004).

### Immunoprecipitation (IP) and mass spectrometry analysis

IP of Pcl2-FLAG from ES cell nuclear extracts using the mouse M2 FLAG antibody (Sigma) and mass spectrometry analysis were carried out as previously described (van den Berg et al., 2010).

### Chromatin Immunoprecipitation (ChIP) and gene expression analysis

Cells were fixed in suspension in 1% formaldehyde for 10 minutes, quenched with 125 mM glycine for 5 minutes and lysed in 1% SDS, 10 mM EDTA pH 8.0, 50 mM Tris-HCl pH 8.1 and protease inhibitors for 10 minutes at 4°C. Chromatin was fragmented to 0.3-0.5 kb by sonication. One hundred and fifty micrograms of chromatin was used per IP. Chromatin was diluted 1:10 in 1% Triton X-100, 2 mM EDTA pH 8.0, 150 mM NaCl, 20 mM Tris-HCl pH 8.1, protease inhibitors and pre-cleared with 30 μl of protein A or G agarose beads (Millipore) for 90 minutes at 4°C. Chromatin was subjected to IP overnight at 4°C using 5 μl of the following antibodies: anti-Ezh2 (Diagenode), anti-Suz12 (Diagenode), anti-H3K27me3 (Millipore) and anti-H3K4me3 (Millipore). For all experiments, 2 μl of anti-mouse IgG (Sigma) was used to measure background levels and 2 μl of anti-histone H3 (Abcam) served as input control. Thirty microlitres of protein G or protein A agarose beads were used to pull down immunocomplexes for 2 hours at 4°C. DNA was reverse crosslinked, eluted in 1% SDS, 0.1 M $NaHCO_3$ and precipitated with isopropanol. DNA was resuspended in 100 μl $H_2O$ and analysed by real-time PCR using SYBR Green PCR Master Mix (Bio-Rad) following the manufacturer's instructions, on a Chromo4 real-time PCR system (Bio-Rad). Enrichment was normalised to 10% of input DNA.

For FLAG ChIP, following fixation as above cells were washed once in 10 mM Hepes pH 7.5, 200 mM NaCl, 1 mM EDTA, 0.5 mM EGTA, protease inhibitors and lysed in 25 mM Tris pH 7.5, 150 mM NaCl, 5 mM

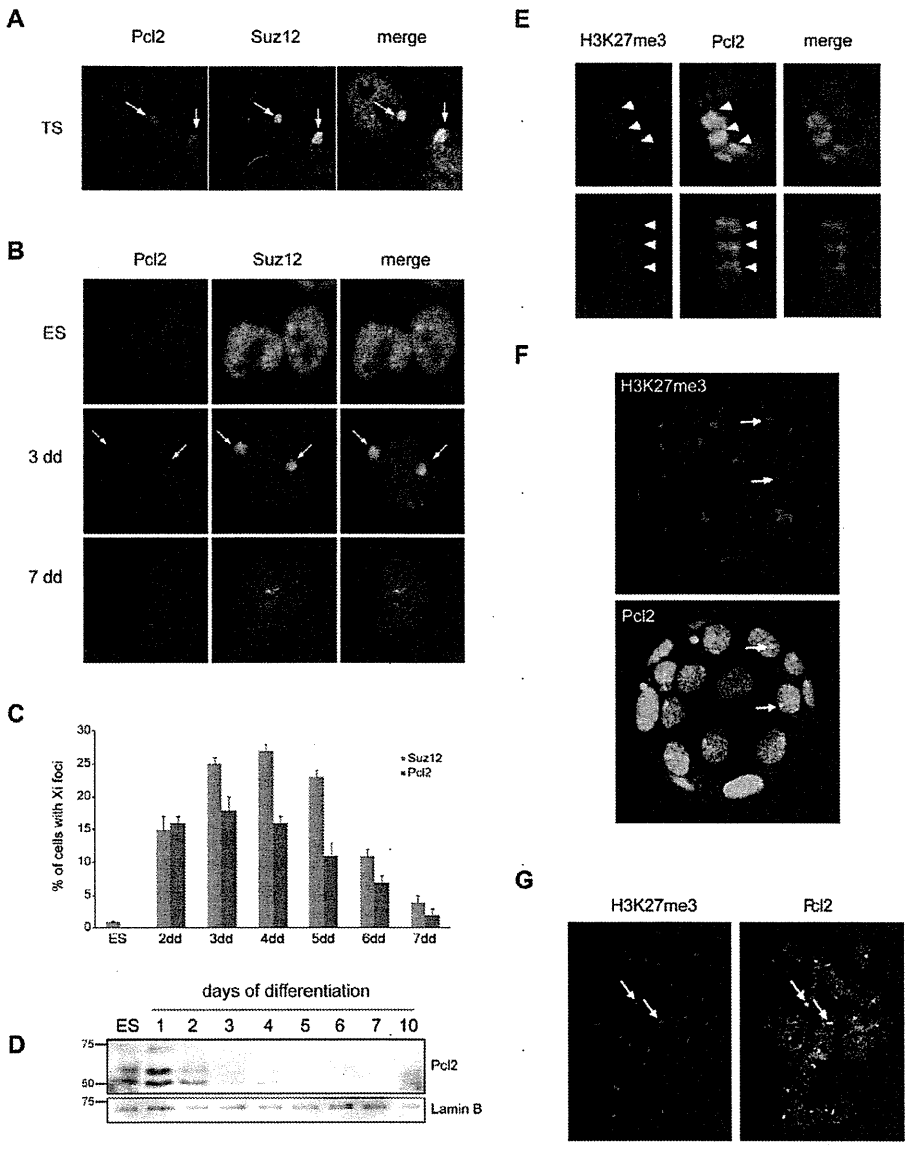


**Fig. 1. Pcl2 is enriched on the inactive X chromosome (Xi) in vitro and in vivo.** (**A**) Pcl2 localises to the Xi in mouse trophoblast stem (TS) cells. Example of immunofluorescence (IF) analysis in XX B1 TS cells using anti-Pcl2 and anti-Suz12 antibodies, showing colocalisation in Xi domains (arrows). (**B**) Example of IF analysis of Suz12 and Pcl2 (arrows) in undifferentiated XX ES cells (ES) and in ES cells differentiated for 3 (3 dd) or 7 (7 dd) days. (**C**) Quantitative scoring results illustrate the proportion of cells with Xi foci detected with anti-Suz12 and anti-Pcl2 antibodies for undifferentiated ES cells (ES) and cells differentiated for 2-7 days. A minimum of 234 cells was scored for each time point. Error bars represent the s.d. between replicates. (**D**) Western blot of nuclear extracts from undifferentiated ES cells (ES) and cells differentiated for 1-7 and 10 days and analysed by western blot using antibodies against Pcl2 and lamin B (loading control). The Pcl2 antibody reproducibly detects three major Pcl2 isoforms at 52, 60 and 68 kDa (see Li et al., 2011). (**E**) Examples of IF showing colocalisation of Pcl2 and H3K27me3 in a banded pattern (arrowheads) on the Xi at metaphase. (**F,G**) Pcl2 localises to the Xi in preimplantation (F) and postimplantation (G) XX embryos. Examples illustrate colocalisation of H3K27me3 (red) and Pcl2 (green) to Xi domains (arrows).

EDTA, 1% Triton X-100, 0.1% SDS, 0.5% sodium deoxycholate, protease inhibitors. One hundred and fifty micrograms of chromatin was used for IP with 5 μl M2 FLAG antibody (Sigma) overnight at 4°C, and subsequently with 30 μl of protein A or G agarose beads for 2 hours at 4°C.

Each ChIP experiment was performed independently three times. Primers used are shown in Table S4 in the supplementary material. RT-PCR for PcG target loci was carried out using standard methods and primers are listed in Table S5 in the supplementary material.

### Gel filtration analysis

For Pcl2-PRC2 complex analysis (Fig. 2D), a Superose 6 SMART gel filtration column (GE Healthcare) was pre-calibrated with the gel filtration standards thyroglobin (669 kDa), γ-globulin (158 kDa), ovalbumin (44 kDa), myoglobulin (17 kDa) and vitamin B12 (1.35 kDa) (Bio-Rad). Purified Pcl2-FLAG complex obtained by IP was loaded onto the column pre-equilibrated with the buffer used for IP. Fractions were collected at a flow rate of 40 μl/minute and analysed by western blotting.

For gel filtration of PRC2 complexes in nuclear extracts, 4 μg of high-salt nuclear extracts from ES cells were loaded on a Superose 6 SMART gel filtration column pre-equilibrated with low-salt buffer (10% glycerol, 40 mM Hepes pH 7.6, 150 mM KCl, 0.5 mM EDTA, 1 mM DTT). Fifty-two fractions of 250 μl were collected and analysed by western blotting. Prior to the assay, the column was pre-calibrated using the gel filtration standards Blue Dextran 2000 (2 MDa), thyroglobin, apoferritin (440 kDa), γ-globulin, conalbumin (75 kDa) and ovalbumin (GE Healthcare).

## RESULTS

### Transient enrichment of Pcl2 on the Xi at the onset of X inactivation

We set out to investigate whether mammalian Pcl proteins play a role in X chromosome inactivation, building on previous observations demonstrating that the Xi is an important PcG target (Mak et al., 2002; Silva et al., 2003; de Napoles et al., 2004). We first carried out indirect immunofluorescence (IF) experiments in XX (female) trophoblast stem (TS) cells using an antibody specific for mouse Pcl2 (Li et al., 2011). Pcl2 was found to be diffusely localised throughout much of the nucleoplasm and, in addition, was highly enriched in a single domain that colocalised with a concentrated signal for the core PRC2 protein Suz12, a defined

marker of the Xi chromosome (Fig. 1A). No focal Pcl2 staining was observed in XY TS cells (data not shown). Thus, Pcl2 is concentrated on the Xi chromosome in a similar manner to core components of both PRC1 and PRC2 complexes.

TS cells provide an in vitro model for the imprinted form of X inactivation that occurs in extraembryonic lineages of mouse embryos. To test for an involvement of Pcl2 in the random form of X inactivation we analysed differentiating XX mouse ES cells. Previous studies have demonstrated that modification of Xi chromatin in this model system occurs in a progressive, stepwise process that is initiated by an accumulation of Xist RNA (reviewed by Heard, 2005). Recruitment of PRC2 and PRC1 complexes and accumulation of the associated histone modifications H3K27me3 and H2AK119ub1 occur early, immediately following the onset of *Xist* expression (Mak et al., 2002; Silva et al., 2003; de Napoles et al., 2004). The accumulation of PRC1 and PRC2 proteins on the Xi diminishes as differentiation proceeds, but low or moderate levels are presumably maintained as both H3K27me3 and H2AK119ub1 persist (Silva et al., 2003; de Napoles et al., 2004). To study nuclear localisation of Pcl2 in random X inactivation, XX ES cells were differentiated in vitro for 7 days, and samples corresponding to each day of differentiation were analysed by indirect IF using Pcl2- and Suz12-specific antibodies (Fig. 1B). Pcl2 staining closely mirrored that seen for Suz12. Xi foci were not detected in undifferentiated cells, consistent with both X chromosomes being active. However, strong Xi foci were seen in early-stage differentiated cells and the localised signal diminished progressively as differentiation proceeded (Fig. 1C). Pcl2 foci were undetectable in XX mouse embryo fibroblast (MEF) cell lines known to have an Xi (not shown), similar to results previously reported for core PRC2 proteins (Plath et al., 2003; Silva et al., 2003). Consistent with these observations, western blot analysis (Fig. 1D) and quantitative RT-PCR (see Fig. S1A in the supplementary material) demonstrated that Pcl2 is highly expressed in undifferentiated ES cells and during early stages of differentiation and that levels drop rapidly at later differentiation stages (Fig. 1D and see Fig. S1B in the supplementary material).

In a proportion of mitotic cells, Pcl2 staining was observed on a single condensed chromosome, presumably the Xi (Fig. 1E). This signal was localised in a characteristic banded pattern observed previously for Xist RNA (Duthie et al., 1999) and PcG core components or associated histone modifications (Mak et al., 2002; de Napoles et al., 2004). Together, these results demonstrate that Pcl2 is enriched on Xi and that Pcl2 recruitment coincides with early stages of X inactivation in vitro.

To assess the accumulation of Pcl2 on Xi in vivo during normal development, IF analysis was carried out on mouse embryos using antibodies to H3K27me3 to counterstain the Xi. In blastocysts (E3.5), in which X inactivation is paternally imprinted (Mak et al., 2004), Pcl2 Xi foci were detected in the majority of cells in approximately half of all embryos examined (presumptive XX versus XY embryos) (Fig. 1F). At earlier preimplantation stages we failed to detect Pcl2 Xi foci, similar to results obtained previously for PRC2 core proteins (Mak et al., 2004; Okamoto et al., 2004). To examine Pcl2 association with Xi in random X inactivation we carried out IF on dissociated embryonic cells from individual XX postimplantation embryos. Pcl2 Xi foci were detected in the majority of cells at E6.5 and E7.5 (Fig. 1G), but not in later-stage embryos. This again mirrors the results obtained for core PRC2 proteins, in which enrichment on Xi is only observed during a developmental window when levels of the proteins are high (Mak et al., 2002; Silva et al., 2003; de Napoles et al., 2004). In summary, Pcl2 is enriched on the Xi chromosome specifically during those developmental stages at which PRC2 proteins were shown to be recruited to the Xi.

## Pcl2 in mouse ES cells forms a stable complex with core PRC2 proteins

Biochemical purification of the *Drosophila* Polycomblike protein and of the human Polycomblike homologue PHF1 (PCL1) demonstrated an interaction with the PRC2 complex (O'Connell et al., 2001; Nekrasov et al., 2007; Cao et al., 2008; Sarma et al., 2008). To determine whether Pcl2 associates with PRC2 components, we purified FLAG-tagged Pcl2 (Pcl2-FLAG) from ES cells and analysed the purified fractions by western blot and mass spectrometry. PGK12.1 ES cells stably expressing Pcl2-FLAG were characterised and we selected two clones, B2 and E1, that expressed full-length Pcl2-FLAG at levels similar to endogenous Pcl2 (Fig. 2A). Analysis of the distribution of Pcl2-FLAG in nuclear fractions revealed an identical distribution to that of endogenous Pcl2, being found predominantly in S3, the high-salt fraction (Fig. 2B).

Pcl2-FLAG protein was immunoprecipitated using anti-FLAG agarose beads from nuclear extracts of PGK12.1 Pcl2-FLAG cell lines and eluted with FLAG tri-peptide. Non-transfected PGK12.1 ES cells were used as a control. Western blot analysis revealed that Pcl2-FLAG co-immunoprecipitates with the core PRC2 components Ezh2, Suz12 and Eed isoform 3, the most abundant isoform in mouse ES cells (Fig. 2C). The chromatin protein YY1, which was used as a negative control, was not detected. Pcl2-FLAG did not significantly deplete the pool of PRC2 proteins, as indicated by retention of signal in the flow-through fractions (Fig. 2C, Ft), suggesting that Pcl2-PRC2 complexes represent a relatively small proportion of the cellular PRC2 complement.

Mass spectrometry analysis was carried out on Pcl2-FLAG immunoprecipitation (IP) fractions to identify proteins that co-purify. Fig. 2E and Table S1 in the supplementary material summarise the data obtained from three independent IP experiments. The PRC2 proteins Ezh2, Suz12 and Eed, which constitute the catalytic core of the complex, were detected in all three experiments, as was Pcl2. RbAp46 and RbAp48, which have previously been shown to co-purify with PRC2, were not detected consistently, although RbAp48 was found in one experiment. No other proteins gave a high mascot score (>500) in more than one experiment (see Table S1 in the supplementary material), suggesting that the Pcl2-PRC2 complex does not have additional components.

To further analyse Pcl2-PRC2 subunit composition, Pcl2-FLAG IP fractions were analysed by size exclusion chromatography on a Superose 6 column. Previous studies have estimated the size of the core PRC2 complex purified from *Drosophila* and mammalian cells to be ~550-600 kDa (Kuzmichev et al., 2002; Nekrasov et al., 2005; Sarma et al., 2008) and that Pcl-PRC2 and PHF1-PRC2 purified from *Drosophila* embryos and Hela cells, respectively, sediment at ~600 kDa (Nekrasov et al., 2007; Cao et al., 2008; Sarma et al., 2008). Consistent with these findings, we detected Pcl2-FLAG and Suz12 proteins in fractions corresponding to ~600 kDa (Fig. 2D).

## Pcl2 modulates the biochemical properties of PRC2 complexes and facilitates PRC2 recruitment to the Xi

To analyse the function of Pcl2 we established ES cell lines in which Pcl2 expression was stably knocked down by shRNA. A number of constructs expressing shRNAs that target different parts

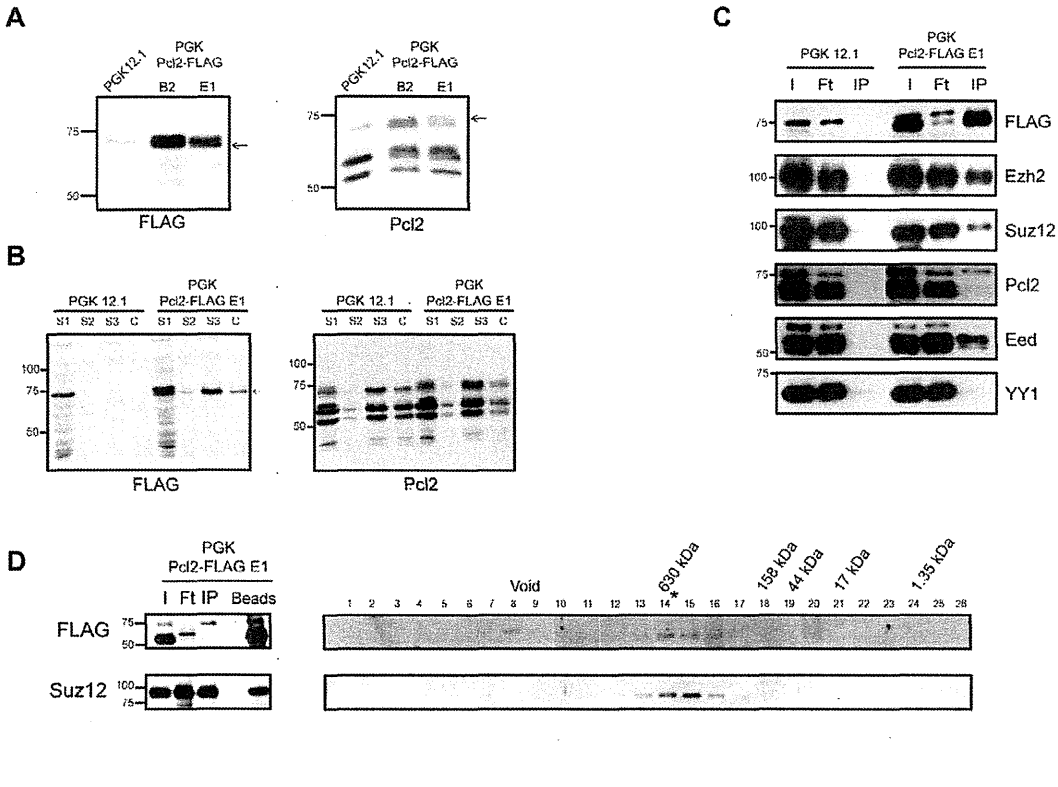


E

| | 2xFLAG-Pcl2 | | |
|---|---|---|---|
| | Unique peptides IP1-IP2-IP3 | Mascot Score IP1-IP2-IP3 | Coverage (%) IP1-IP2-IP3 |
| **Suz12** | 23-23-16 | 1603-1778-1202 | 51.1-49.4-33.2 |
| **Ezh2** | 18-18-2 | 1257-1160-62 | 37.8-36.5-2.5 |
| **Eed** | 12-14-8 | 845-761-411 | 25.8-27.9-19.1 |
| **Pcl2** | 12-8-2 | 745-485-182 | 26.5-15.3-11.5 |
| **Rbbp7** | 9-0-0 | 567-0-0 | 30.1-0-0 |

**Fig. 2. Biochemical analysis of Pcl2 and its interaction with PRC2.** (**A**) Stable expression of Pcl2-FLAG in mouse ES cells. Cell lysates prepared from PGK12.1 ES cells and two derivative cell lines stably expressing Pcl2-FLAG (B2 and E1) were analysed by western blot using anti-FLAG or anti-Pcl2 antibodies. Recombinant Pcl2-FLAG is indicated with arrows. (**B**) Western blot using anti-FLAG or anti-Pcl2 antibodies illustrating that Pcl2 and Pcl2-FLAG are predominantly in the high-salt nuclear fractions from PGK12.1 and PGK Pcl2-FLAG ES clone E1. S1 corresponds to the cytoplasmic fraction, S2 to low-salt nuclear extract, S3 to high-salt nuclear extract, and C to chromatin-bound fraction. (**C**) FLAG immunoprecipitation (IP) from PGK12.1 ES cells and PGK Pcl2-FLAG clone E1 illustrating that PRC2 core components co-immunoprecipitate with recombinant Pcl2-FLAG. The input fraction (I) corresponding to the initial nuclear extract, flow-through (Ft) and elution fraction (IP) from FLAG purification of clone E1 were analysed by western blot using anti-FLAG and antibodies to assess co-IP with Ezh2, Suz12, Pcl2, Eed and YY1. (**D**) Size exclusion chromatography of Pcl2-PRC2 purified by FLAG IP from PGK Pcl2-FLAG clone E1. Input (I), flow-through (Ft), elution fraction (IP) and beads were analysed prior to gel filtration by western blot with anti-FLAG, anti-Ezh2 and anti-Suz12 antibodies to confirm efficient pull-down (left). IP fraction was loaded on a Superose 6 SMART column. Fractions 1-26 were analysed by western blotting with antibodies against FLAG, Ezh2 and Suz12 (right). Asterisk indicates peak fraction. Molecular weight standards used to calibrate the column and void volume are indicated at the top. (**E**) Mass spectrometry of Pcl2-FLAG immunoprecipitates from three independent experiments (IP1, IP2 and IP3) identified core PRC2 proteins. The number of unique peptides, the protein identification score (Mascot) and protein coverage are shown.

of the *Pcl2* transcript were transfected into PGK12.1 XX cells. Two shRNAs, CL3.5 and CL4, that resulted in a clear reduction in Pcl2 protein levels in a number of independent clones (see Fig. S2 in the supplementary material) were selected for further analysis.

We initially assessed PRC2 complexes in nuclear extracts from wild-type and knockdown cell lines using size exclusion chromatography. As shown in independent experiments (Fig. 3A and see Fig. S2C in the supplementary material), Pcl2 and the core PRC2 components Ezh2 and Suz12 co-elute in a major peak of 600-700 kDa (centred on fraction 21) and as high molecular weight complexes of 1-2 MDa (fractions 3-15). In Pcl2-depleted nuclear extracts we observed a shift in the size distribution of the major peak to ~500-550 kDa and a reduction in the abundance of the high molecular weight PRC2 complexes. Rbpj, a chromatin factor that is not associated with PRC2, eluted at equivalent fractions in both control and Pcl2-depleted nuclear

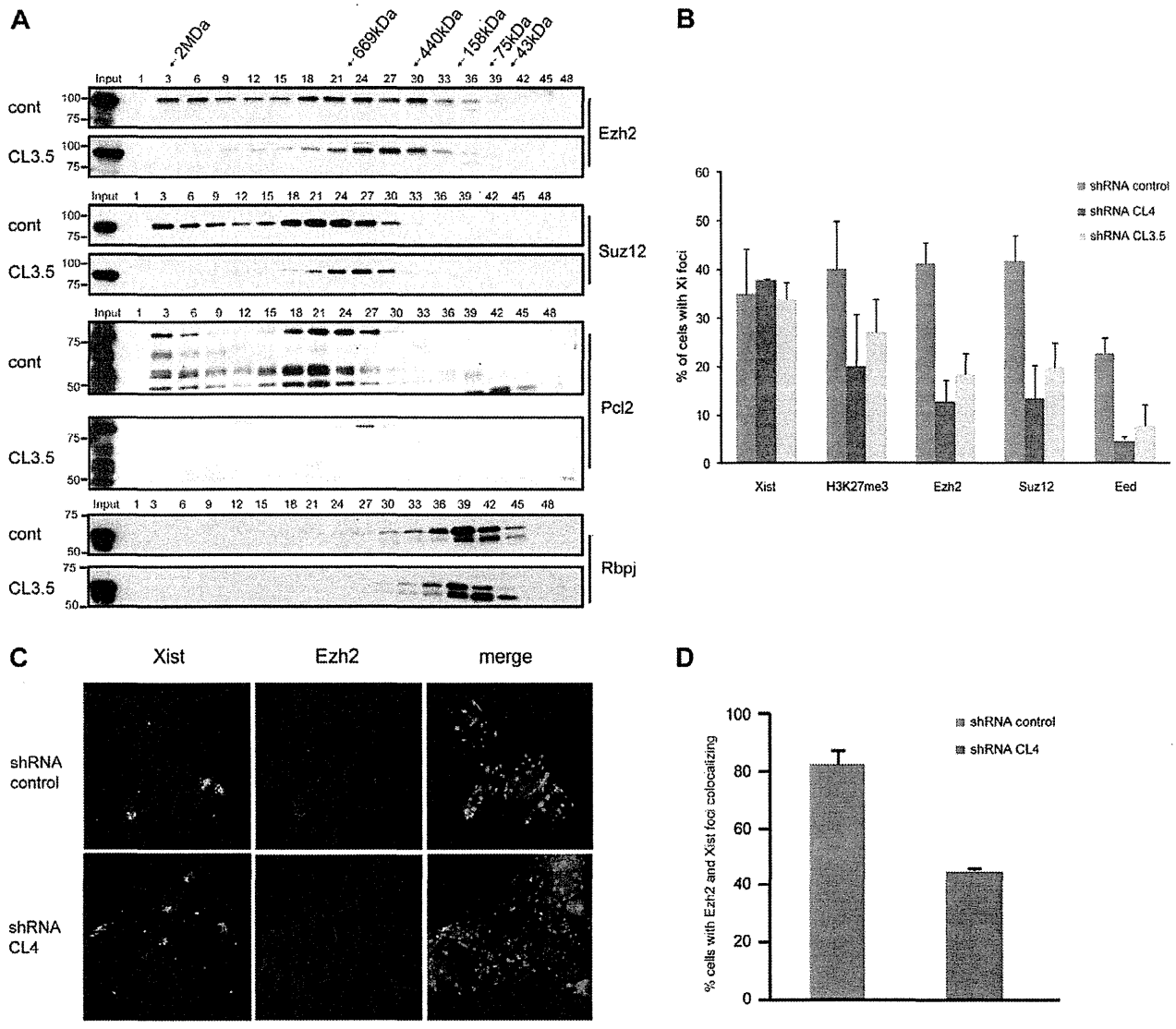


**Fig. 3. Pcl2 depletion affects high molecular weight PRC2 complexes in ES cells and impairs recruitment of PRC2 to the Xi.** (**A**) Nuclear extracts from mouse PGK12.1 cells and Pcl2 shRNA clone 3.5 were loaded on a Superose 6 gel filtration column and fractionated. One in every three fractions was run on an SDS-PAGE gel and analysed by western blot using anti-Ezh2, anti-Suz12 anti-Pcl2 and anti-Rbpj antibodies. (**B**) Xist RNA fluorescent in situ hybridisation (FISH) and IF detection of H3K27me3, Ezh2, Suz12 and Eed were performed in one control (blue bars) and two Pcl2 shRNA (red and green bars) cell lines differentiated in vitro for 3 days. The mean + s.d. ($n$=3) of the percentage of cells for which Xi foci could be observed is represented. At least 100 cells were scored per slide. (**C**) Examples of immuno-RNA FISH analysis of Ezh2 and Xist RNA in control and Pcl2 shRNA cell lines in 3-day differentiated XX ES cells. (**D**) Colocalisation of Xist and Ezh2 Xi domains, showing the percentage of cells with Xist RNA domains that had colocalising Ezh2 foci (control, $n$=80; Pcl2 shRNA, $n$=47). Error bars represent the s.d. between replicates.

extracts (Fig. 3A). The size shift seen for the major PRC2 peak might be attributable to the absence of Pcl2, although this seems unlikely given that Pcl2-PRC2 represents only a relatively small fraction of total PRC2 (Fig. 2C).

We went on to test the role of Pcl2 in PRC2 function in X chromosome inactivation. Indirect IF analysis was carried out using antibodies against Ezh2, Eed, Suz12 and H3K27me3 on two independent PGK12.1 Pcl2 shRNA ES cell lines and a control cell line differentiated in vitro for 3 days, a timepoint at which *Xist* upregulation and PRC2 recruitment to the Xi have occurred in a significant proportion of cells (Sheardown et al., 1997; Silva et al., 2003). We also analysed Xist RNA expression by RNA fluorescent in situ hybridisation (FISH) to exclude indirect effects on *Xist* expression or cell differentiation. For each experiment, the number of foci corresponding to the Xi was counted and divided by the total number of cells analysed. We observed a strong reduction in the number of cells with Xi domains detected using antibodies to Suz12, Ezh2 and Eed in both PGK12.1 Pcl2 shRNA clones relative to the shRNA control cell line (Fig. 3B). H3K27me3 Xi domains were also reduced in Pcl2 knockdown cells, although to a lesser extent. Robust Xist RNA domains were observed in ~35% of cells in all cases, which

is similar to the frequency observed for PGK12.1 cells in previous studies (Sheardown et al., 1997), indicating that reduced PRC2 recruitment is not due to indirect effects.

To confirm these observations we carried out dual IF/RNA FISH analysis to detect both Ezh2 and Xist RNA in control and Pcl2 knockdown cells. Xist domains depleted for Ezh2 staining were detected in a significant proportion of Pcl2 knockdown cells when compared with wild-type controls (Fig. 3C,D). These observations demonstrate that Pcl2 has a role in the recruitment and/or maintenance of PRC2 on the Xi.

### Pcl2 is important for the recruitment of PRC2 to Polycomb targets in ES cells

Recruitment of PRC2 complexes to Xi is dependent on Xist RNA (Mak et al., 2002; Silva et al., 2003) and the importance of Pcl2 in this process might constitute a specialised function. To explore this further, we analysed the role of Pcl2 at other known PcG target loci. Recent studies have demonstrated that, in undifferentiated ES cells, PcG complexes collaborate to repress a large number of genes that encode master regulators of embryonic and extraembryonic lineages (Boyer et al., 2006; Bracken et al., 2006; Lee et al., 2006). The promoters of many of these target genes exhibit an unusual chromatin configuration, termed bivalent chromatin, showing an enrichment for PcG-mediated repressive histone modifications, together with histone modifications that mediate transcriptional activity, such as H3K4me3 and H3/H4 acetylation (Azuara et al., 2006; Bernstein et al., 2006). Moreover, bivalent domains are associated with the presence of poised RNA polymerase II (Stock et al., 2007).

To determine whether Pcl2 localises to the promoters of known PRC2 target genes in ES cells, we carried out ChIP analysis. The Pcl2 antibody described above is not suitable for ChIP (data not shown), and we therefore carried out experiments using anti-FLAG antibody in PGK12.1 ES cell lines stably expressing Pcl2-FLAG. ChIP analysis for the histone modification H3K27me3 was carried out in parallel (Fig. 4A). We tested a number of known PcG target loci that encode regulators of extraembryonic and embryonic lineages. As a negative control we analysed *Oct4* (*Pou5f1* – Mouse Genome Informatics), which encodes a transcription factor that is highly expressed in ES cells, and the housekeeping gene beta-2 microglobulin (*B2m*). As expected, H3K27me3 levels were enriched at the promoters of PcG target loci but not at promoters of genes expressed in ES cells. Pcl2-FLAG was also enriched at these loci, with the relative level of enrichment at individual promoters closely mirroring that seen for H3K27me3. This result suggests that Pcl2-PRC2 localises to PRC2 target genes.

To investigate the function of Pcl2 at target loci in ES cells, we assessed levels of H3K27me3, H3K4me3 and of PRC2 core components in Pcl2 knockdown cell lines (Fig. 4B). We observed slightly reduced levels of both H3K27me3 and H3K4me3, although this varied between cell lines. Similarly, global levels of H3K27 and H3K4 methylation, as assessed by western blot analysis, were not significantly affected in the Pcl2 shRNA cell lines (Fig. 4C). In marked contrast, target occupancy of the PRC2 core components Ezh2 and Suz12 was strongly reduced in Pcl2 knockdown cell lines (Fig. 4B). We presume that the reduced PRC2 occupancy at target loci in Pcl2 knockdown cells is nevertheless sufficient to attain near normal levels of H3K27me3. Taken together, these results suggest that Pcl2 facilitates PRC2 recruitment to target loci.

We went on to determine whether Pcl2 knockdown results in the derepression of PRC2 target genes, as occurs in cells lacking core PRC2 proteins (Azuara et al., 2006; Boyer et al., 2006; Lee et al., 2006; Pasini et al., 2007). *Pcl2* transcript levels were clearly reduced in the knockdown cell lines, as expected, but we did not detect elevated expression of the PcG target genes analysed (see Fig. S3 in the supplementary material). This is consistent with the relatively small decrease in H3K27me3 observed at target loci (Fig. 4B). In summary, Pcl2 plays a role in the recruitment of PRC2 complexes to target loci in ES cells. Whereas Pcl2 depletion significantly reduces PRC2 occupancy, H3K27me3 levels are only marginally affected and target genes remain fully repressed.

### PRC2 targeting in ES cells requires the PHD2 domain of Pcl2

Pcl protein and the three mammalian homologues are characterised by the presence of a Tudor domain in the N-terminal region and two centrally located Plant Homeodomain (PHD) fingers (Lonie et al., 1994; O'Connell et al., 2001; Wang, S. et al., 2004). PHD and Tudor domains are found in many chromatin proteins, where they mediate interactions with histones (and other proteins), often through binding specific methylated residues (Bienz, 2006; Mellor, 2006). Previous studies have suggested that the PHD domains of Pcl are required for the interaction with E(z) in *D. melanogaster* (O'Connell et al., 2001). To determine the domain requirements for Pcl2 interactions with PRC2 and for the PRC2 targeting function we derived ES cell lines that express Pcl2-FLAG with or without specific domains (Fig. 5A and see Fig. S4 in the supplementary material) and carried out co-IP and ChIP analyses.

Pcl2-FLAG constructs lacking the Tudor (ΔT), PHD1 (ΔPHD1), PHD2 (ΔPHD2) or both PHD domains (ΔPHD1+2) were generated and transfected into PGK12.1 ES cells and stable cell lines that expressed the mutant proteins were selected (Fig. 5A and see Fig. S4 in the supplementary material). The Pcl2ΔPHD2 construct was poorly expressed in all cell lines tested (see Fig. S4 in the supplementary material) and was therefore excluded from subsequent analyses. To determine which domains of Pcl2 are important for interaction with PRC2 core components, the mutant Pcl2-FLAG proteins were immunoprecipitated using an anti-FLAG antibody bound to agarose beads and eluted using FLAG peptides. Western blot analysis was performed using antibodies to FLAG, Ezh2 and HP1γ (Cbx3 – Mouse Genome Informatics), the latter providing a negative control. The results demonstrated that all Pcl2 deletion mutants efficiently co-immunoprecipitate Ezh2, indicating that other regions of Pcl2 must be important for the interaction with PRC2 core components (Fig. 5B).

We then examined whether the Tudor and/or PHD domains of Pcl2 play a role in its localisation to the promoters of PRC2 target genes by performing ChIP on the cell lines described above. Consistent with the observations made for the full-length Pcl2-FLAG cell line, H3K27me3 levels were enriched at the promoters of target loci in all cell lines analysed. ΔT Pcl2-FLAG and ΔPHD1 Pcl2-FLAG localised at target loci similar to wild-type Pcl2-FLAG (Fig. 5C). By contrast, ΔPHD1+2 Pcl2-FLAG localisation was strongly impaired. These observations suggest that the PHD2 domain of Pcl2 is crucial for mediating PRC2 recruitment/stabilisation at target loci.

## DISCUSSION

In this study we have shown that Pcl2, one of three mammalian homologues of *Drosophila* Pcl, is expressed predominantly in early development and that it forms a stable complex with the core PRC2 polycomb proteins Ezh2, Suz12 and Eed. We demonstrate that this complex, Pcl2-PRC2, plays an important role in the recruitment and/or

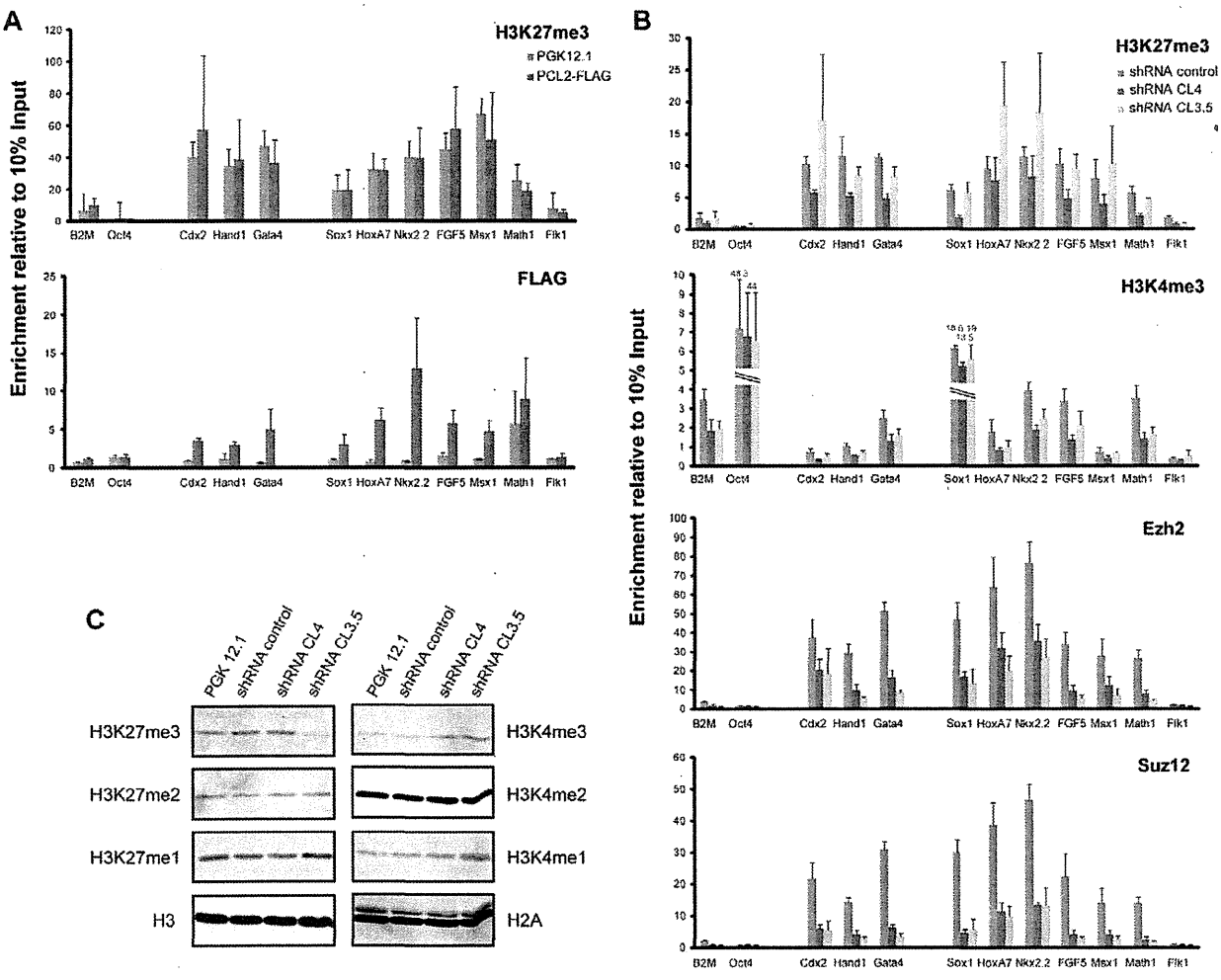


**Fig. 4. Pcl2 localises to PcG target genes in ES cells and facilitates PRC2 recruitment.** (**A**) Pcl2 recruitment to the promoters of various mouse genes was analysed by FLAG ChIP using the M2 FLAG antibody in PGK12.1 cells (blue bars) and PGK Pcl2-FLAG clone E1 (red bars). H3K27me3 enrichments were also measured using the same protocol. Enrichments for each modification analysed by real-time PCR are presented as the mean of three independent ChIP experiments (+ s.d.) and are expressed relative to one-tenth of the input DNA. Genes analysed are arranged in three groups: control expressed genes (*B2m*, *Oct4*), and silent PcG target genes that are normally expressed in extra-embryonic (*Cdx2*, *Hand1*, *Gata4*) or embryonic [*Sox1*, *Hoxa7*, *Nkx2.2*, *Fgf5*, *Msx1*, *Math1* (*Atoh1*), *Flk1* (*Kdr*)] lineages. (**B**) Levels of H3K27me3 and H3K4me3 modifications and recruitment of Ezh2 and Suz12 to promoters of various genes were analysed by ChIP in one control clone and two Pcl2 shRNA cell lines. The loci tested are arranged as above. Enrichments for each modification as assessed by real-time PCR are presented as the mean of three independent experiments (+ s.d.) and are expressed relative to one-tenth of the input DNA. (**C**) Western blot analysis of acid-extracted histones from PGK12.1 ES cells, one shRNA control clone and two Pcl2 shRNA cell lines using antibodies for specific histone modifications as indicated. Histone H3 and H2A blots provide loading controls.

stabilisation of PRC2 both on the Xi and at PcG target genes in ES cells. The PRC2 targeting activity of Pcl2-PRC2 is critically dependent on PHD finger domain 2, suggesting that Pcl2 might function through the recognition of a specific chromatin configuration.

Pcl2 is highly expressed in early development and in ES cells, suggesting that it contributes to PcG function at these stages. In the case of ES cells there is evidence that *Pcl2* is a direct target of the pluripotency factors Oct4 and Nanog (Loh et al., 2006; Walker et al., 2007), and this is likely to be important in determining the Pcl2 expression pattern. The PRC2 protein Eed has similarly been shown to be a direct target of the ES cell transcription factor circuitry (Ura et al., 2008).

Our data suggest that high-level expression of Pcl2 in ES cells and in early embryogenesis is necessary to support the function of PRC2 core complexes in repressing PcG target loci, notably the key lineage determinants defined as PcG targets in ES cells (Boyer et al., 2006; Mikkelsen et al., 2007). A recent report investigating Pcl2 function in ES cells also demonstrated a role for Pcl2 in PRC2 targeting (Walker et al., 2010) and, in addition, found that depletion of Pcl2 enhances the self-renewal characteristics of ES cells and inhibits their differentiation. Our study did not directly address the latter, although we note that in our experiments Pcl2 knockdown did not overtly inhibit differentiation as assessed by embryoid body formation and induction of Xist RNA expression, the latter being

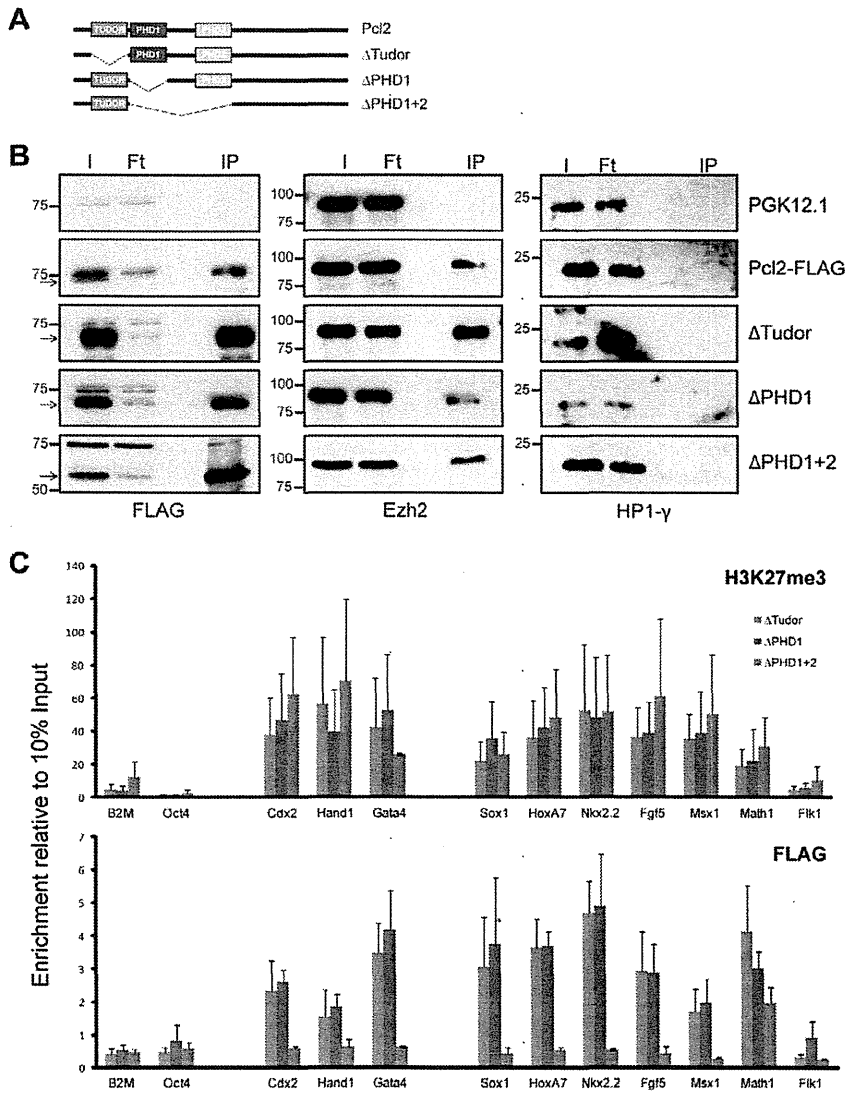


**Fig. 5. The PHD2 domain of Pcl2 is required for recruitment to PcG target genes in ES cells.** (**A**) The Pcl2 deletion mutants analysed. (**B**) Input (I), flow-through (Ft) and elution (IP) fractions from FLAG immunoprecipitates from the three selected mutant cell lines (ΔTudor, ΔPHD1, ΔPHD1+2) were analysed by western blot using anti-FLAG, anti-Ezh2 and anti-HP1γ. IPs from PGK12.1 control cells and PGK Pcl2-FLAG clone E1 are shown for comparison. (**C**) Recruitment of Pcl2 mutant proteins to the promoters of mouse target genes was analysed by FLAG ChIP using selected clones (see Fig. S4 in the supplementary material). H3K27me3 levels were also measured using the same protocol. Enrichments analysed by real-time PCR are presented as the mean of three independent ChIP experiments (+ s.d.) and expressed relative to one-tenth of the input DNA. Genes analysed are arranged as in Fig. 4.

directly linked to the suppression of the pluripotency transcription factor network (Navarro et al., 2008). These differences might be attributable to shRNA-mediated knockdown efficiency or the different ES cell lines used in the respective studies.

PRC2 levels and, more notably, H3K27me3 were only partly reduced following Pcl2 depletion in ES cells and there was no derepression of PcG target loci as has been reported following knockout of PRC2 core components (Azuara et al., 2006; Boyer et al., 2006; Pasini et al., 2007). Moreover, a previous study demonstrated that Pcl2-deficient mice show only mild phenotypes – specifically, minor posterior skeletal transformations (Wang et al., 2007). By contrast, *Drosophila Pcl* mutant embryos exhibit a strong phenotype and early embryo lethality (Duncan, 1982; Breen and Duncan, 1986). A likely explanation for the mild phenotype of mouse *Pcl2* mutants is that the other Pcl homologues, Pcl1 and Pcl3 (Phf1 and Phf19 – Mouse Genome Informatics), functionally compensate for Pcl2 depletion. It will be important in future to address this point, for example by analysing combined knockout animals and/or ES cells.

The initial observation that Pcl2 localises to the Xi chromosome led us to consider that it might be important for Xist RNA-dependent recruitment of PRC2 during X inactivation. The Pcl proteins have two PHD finger domains and a Tudor domain, the latter being found in a number of proteins involved in RNA biogenesis and processing. We observed that the second PHD finger domain is important for PRC2 occupancy at target loci in ES cells. Based on the known function of PHD finger domains (Bienz, 2006; Mellor, 2006), this suggests that Pcl2 might recognise a specific chromatin configuration or histone modification landscape. The function of the other conserved domains of Pcl2 (Tudor and PHD1) is not apparent from our studies, although neither appears to be essential for complex formation or PRC2 occupancy at the target loci we analysed. We cannot rule out the possibility that these domains facilitate the recruitment of PRC2 to other PcG targets including the Xi chromosome.

The role of Pcl2 in facilitating PRC2 recruitment to the Xi chromosome and at PcG target loci in ES cells could be attributable to a function in the recognition of the primary targeting cues, such

as transcription factors, the chromatin landscape or specific RNAs/RNA-binding proteins, or, alternatively, to a role in retaining or stabilising PRC2 occupancy following initial recruitment. The importance of the latter possibility has been highlighted by recent studies demonstrating that PRC2 occupancy is maintained following removal of an initial recruitment signal (Hansen et al., 2008), and that this might be mediated by a direct interaction of the Eed/Esc protein with H3K27me3 (Margueron et al., 2009). It has been suggested that this feedback mechanism is important for maintaining high levels of H3K27me3 at target loci through S phase and the cell cycle and a similar model could be suggested for Pcl2 function mediated through the recognition of PcG target chromatin configuration via PHD domain 2. This explanation would more readily account for the role of Pcl2 in the recruitment of PRC2 both to Xi, which is thought to involve direct targeting by Xist RNA (Plath et al., 2003; Silva et al., 2003; Kohlmaier et al., 2004), and to target loci in ES cells, at which PRC2 recruitment is more likely to be determined by transcription factor binding and/or chromatin features (Endoh et al., 2008; Margueron et al., 2009).

Affinity purification demonstrated that Pcl2 interacts with the Ezh2, Eed and Suz12 core components of the PRC2 complex in a stable biochemical complex with a molecular weight of ~600 kDa. This is in close agreement with data for Pcl complexes purified from *Drosophila* embryos (Nekrasov et al., 2007) and PHF1 (PCL1) complexes from Hela cells (Cao et al., 2008; Sarma et al., 2008). Similar to these studies, our analysis indicates that the Pcl2-PRC2 complex does not include stoichiometric levels of any other proteins. Jarid2, recently described as a major PRC2 interactor in ES cells, and AEBP2, a zinc-finger protein observed to co-purify with PRC2 in Hela cells and ES cells, were not detected, suggesting that the interaction of these components with PRC2 might be mutually exclusive with that of Pcl2. Consistent with this, a recent study found that Pcl2, Aebp2 and Jarid2 co-purify with the PRC2 core protein Eed from ES cells, but that Pcl2 levels are much lower in complexes that co-purify with Jarid2 (Landeira et al., 2010).

Although purified Pcl2-PRC2 complexes migrate on gel filtration columns with a molecular weight of ~600 kDa, which is similar to that of core PRC2 complexes purified in a number of independent studies, direct gel filtration of ES cell nuclear extracts revealed a size distribution ranging from 600-700 kDa up to 2 MDa. High molecular weight PRC2 species have also been described previously, both in *Drosophila* (Tie et al., 2003) and Hela cells (Kuzmichev et al., 2005). Following depletion of Pcl2 we observed a shift in the size distribution of the major peak to ~500-550 kDa and a reduction in the abundance of the higher molecular weight (1-2 MDa) PRC2 species. One interpretation of this result is that the larger complexes include additional subunits for which recruitment is Pcl2 dependent. Alternatively, high molecular weight species could arise through multimerisation of core PRC2 complexes, an idea favoured by recent studies revealing that the N-terminus of the core PRC2 protein Eed/Esc interacts with histone H3 and dimerises in a phosphorylation-dependent manner (Tie et al., 2005; Margueron et al., 2009). Although we cannot differentiate between these possibilities, the absence of additional stoichiometric components in purified Pcl2-PRC2 and the fact that Pcl2 depletion affects the biochemical properties of total PRC2, only a small proportion of which is associated with Pcl2 at any given time, lead us to favour the idea that Pcl2 mediates the formation of higher-order PRC2 complexes.

In summary, this study highlights Pcl2 as an important PRC2 co-factor that functions in early development and in ES cells to facilitate the recruitment/retention of the complex at target loci.

**Acknowledgements**

We thank Naveenan Navaratnam and Rob Klose for advice on biochemical studies; Amanda Fisher, Stephan Sauer, David Landeira and members of the N.B. lab for valuable feedback and discussion; and Anne-Valérie Gendrel for critical reading of the manuscript. This work was supported by the MRC UK and the Wellcome Trust. M.C. was supported by a D. Phil. GABBA Studentship from the Fundação para a Ciência e Tecnologia, Portugal. Deposited in PMC for release after 6 months.

**Competing interests statement**

The authors declare no competing financial interests.

**Supplementary material**

Supplementary material for this article is available at http://dev.biologists.org/lookup/suppl/doi:10.1242/dev.053652/-/DC1

**References**

**Azuara, V., Perry, P., Sauer, S., Spivakov, M., Jorgensen, H. F., John, R. M., Gouti, M., Casanova, M., Warnes, G., Merkenschlager, M. et al.** (2006). Chromatin signatures of pluripotent cell lines. *Nat. Cell Biol.* **8**, 532-538.

**Bernstein, B. E., Mikkelsen, T. S., Xie, X., Kamal, M., Huebert, D. J., Cuff, J., Fry, B., Meissner, A., Wernig, M., Plath, K. et al.** (2006). A bivalent chromatin structure marks key developmental genes in embryonic stem cells. *Cell* **125**, 315-326.

**Bienz, M.** (2006). The PHD finger, a nuclear protein-interaction domain. *Trends Biochem. Sci.* **31**, 35-40.

**Boyer, L. A., Plath, K., Zeitlinger, J., Brambrink, T., Medeiros, L. A., Lee, T. I., Levine, S. S., Wernig, M., Tajonar, A., Ray, M. K. et al.** (2006). Polycomb complexes repress developmental regulators in murine embryonic stem cells. *Nature* **441**, 349-353.

**Bracken, A. P., Dietrich, N., Pasini, D., Hansen, K. H. and Helin, K.** (2006). Genome-wide mapping of Polycomb target genes unravels their roles in cell fate transitions. *Genes Dev.* **20**, 1123-1136.

**Breen, T. R. and Duncan, I. M.** (1986). Maternal expression of genes that regulate the bithorax complex of Drosophila melanogaster. *Dev. Biol.* **118**, 442-456.

**Cao, R., Wang, L., Wang, H., Xia, L., Erdjument-Bromage, H., Tempst, P., Jones, R. S. and Zhang, Y.** (2002). Role of histone H3 lysine 27 methylation in Polycomb-group silencing. *Science* **298**, 1039-1043.

**Cao, R., Tsukada, Y. and Zhang, Y.** (2005). Role of Bmi-1 and Ring1A in H2A ubiquitylation and Hox gene silencing. *Mol. Cell* **20**, 845-854.

**Cao, R., Wang, H., He, J., Erdjument-Bromage, H., Tempst, P. and Zhang, Y.** (2008). Role of hPHF1 in H3K27 methylation and Hox gene silencing. *Mol. Cell. Biol.* **28**, 1862-1872.

**Chan, C. S., Rastelli, L. and Pirrotta, V.** (1994). A Polycomb response element in the Ubx gene that determines an epigenetically inherited state of repression. *EMBO J.* **13**, 2553-2564.

**Czermin, B., Melfi, R., McCabe, D., Seitz, V., Imhof, A. and Pirrotta, V.** (2002). Drosophila enhancer of Zeste/ESC complexes have a histone H3 methyltransferase activity that marks chromosomal Polycomb sites. *Cell* **111**, 185-196.

**de Napoles, M., Mermoud, J. E., Wakao, R., Tang, Y. A., Endoh, M., Appanah, R., Nesterova, T. B., Silva, J., Otte, A. P., Vidal, M. et al.** (2004). Polycomb group proteins Ring1A/B link ubiquitylation of histone H2A to heritable gene silencing and X inactivation. *Dev. Cell* **7**, 663-676.

**Duncan, I. M.** (1982). Polycomblike: a gene that appears to be required for the normal expression of the bithorax and antennapedia gene complexes of Drosophila melanogaster. *Genetics* **102**, 49-70.

**Duthie, S. M., Nesterova, T. B., Formstone, E. J., Keohane, A. M., Turner, B. M., Zakian, S. M. and Brockdorff, N.** (1999). Xist RNA exhibits a banded localization on the inactive X chromosome and is excluded from autosomal material in cis. *Hum. Mol. Genet.* **8**, 195-204.

**Elderkin, S., Maertens, G. N., Endoh, M., Mallery, D. L., Morrice, N., Koseki, H., Peters, G., Brockdorff, N. and Hiom, K.** (2007). A phosphorylated form of Mel-18 targets the Ring1B histone H2A ubiquitin ligase to chromatin. *Mol. Cell* **28**, 107-120.

**Endoh, M., Endo, T. A., Endoh, T., Fujimura, Y., Ohara, O., Toyoda, T., Otte, A. P., Okano, M., Brockdorff, N., Vidal, M. et al.** (2008). Polycomb group proteins Ring1A/B are functionally linked to the core transcriptional regulatory circuitry to maintain ES cell identity. *Development* **135**, 1513-1524.

**Francis, N. J., Saurin, A. J., Shao, Z. and Kingston, R. E.** (2001). Reconstitution of a functional core polycomb repressive complex. *Mol. Cell* **8**, 545-556.

**Gambetta, M. C., Oktaba, K. and Muller, J.** (2009). Essential role of the glycosyltransferase sxc/Ogt in polycomb repression. *Science* **325**, 93-96.

**Hansen, K. H., Bracken, A. P., Pasini, D., Dietrich, N., Gehani, S. S., Monrad, A., Rappsilber, J., Lerdrup, M. and Helin, K.** (2008). A model for transmission of the H3K27me3 epigenetic mark. *Nat. Cell Biol.* **10**, 1291-1300.

**Heard, E.** (2005). Delving into the diversity of facultative heterochromatin: the epigenetics of the inactive X chromosome. *Curr. Opin. Genet. Dev.* **15**, 482-489.

**Kohlmaier, A., Savarese, F., Lachner, M., Martens, J., Jenuwein, T. and Wutz, A.** (2004). A chromosomal memory triggered by Xist regulates histone methylation in X inactivation. *PLoS Biol.* **2**, E171.
**Kuzmichev, A., Nishioka, K., Erdjument-Bromage, H., Tempst, P. and Reinberg, D.** (2002). Histone methyltransferase activity associated with a human multiprotein complex containing the Enhancer of Zeste protein. *Genes Dev.* **16**, 2893-2905.
**Kuzmichev, A., Margueron, R., Vaquero, A., Preissner, T. S., Scher, M., Kirmizis, A., Ouyang, X., Brockdorff, N., Abate-Shen, C., Farnham, P. et al.** (2005). Composition and histone substrates of polycomb repressive group complexes change during cellular differentiation. *Proc. Natl. Acad. Sci. USA* **102**, 1859-1864.
**Landeira, D., Sauer, S., Poot, R., Dvorkina, M., Mazzarella, L., Jorgensen, H. F., Pereira, C. F., Leleu, M., Piccolo, F. M., Spivakov, M. et al.** (2010). Jarid2 is a PRC2 component in embryonic stem cells required for multi-lineage differentiation and recruitment of PRC1 and RNA Polymerase II to developmental regulators. *Nat. Cell Biol.* **12**, 618-624.
**Lee, T. I., Jenner, R. G., Boyer, L. A., Guenther, M. G., Levine, S. S., Kumar, R. M., Chevalier, B., Johnstone, S. E., Cole, M. F., Isono, K. et al.** (2006). Control of developmental regulators by Polycomb in human embryonic stem cells. *Cell* **125**, 301-313.
**Lewis, E. B.** (1978). A gene complex controlling segmentation in Drosophila. *Nature* **276**, 565-570.
**Li, G., Margueron, R., Ku, M., Chambon, P., Bernstein, B. E. and Reinberg, D.** (2010). Jarid2 and PRC2, partners in regulating gene expression. *Genes Dev.* **24**, 368-380.
**Li, X., Isono, K., Yamada, D., Endo, T. A., Endoh, M., Shinga, J., Mizutani-Koseki, Y., Otte, A. P., Casanova, M., Kitamura, H. et al.** (2011). Mammalian polycomb-Like Pcl2/Mtf2 Is a novel regulatory component of PRC2 that can differentially modulate polycomb activity both at the Hox gene cluster and at Cdkn2a genes. *Mol. Cell. Biol.* **31**, 351-364.
**Loh, Y. H., Wu, Q., Chew, J. L., Vega, V. B., Zhang, W., Chen, X., Bourque, G., George, J., Leong, B., Liu, J. et al.** (2006). The Oct4 and Nanog transcription network regulates pluripotency in mouse embryonic stem cells. *Nat. Genet.* **38**, 431-440.
**Lonie, A., D'Andrea, R., Paro, R. and Saint, R.** (1994). Molecular characterisation of the Polycomblike gene of Drosophila melanogaster, a trans-acting negative regulator of homeotic gene expression. *Development* **120**, 2629-2636.
**Mak, W., Baxter, J., Silva, J., Newall, A. E., Otte, A. P. and Brockdorff, N.** (2002). Mitotically stable association of polycomb group proteins eed and enx1 with the inactive x chromosome in trophoblast stem cells. *Curr. Biol.* **12**, 1016-1020.
**Mak, W., Nesterova, T. B., de Napoles, M., Appanah, R., Yamanaka, S., Otte, A. P. and Brockdorff, N.** (2004). Reactivation of the paternal X chromosome in early mouse embryos. *Science* **303**, 666-669.
**Margueron, R., Justin, N., Ohno, K., Sharpe, M. L., Son, J., Drury, W. J., 3rd, Voigt, P., Martin, S. R., Taylor, W. R., De Marco, V. et al.** (2009). Role of the polycomb protein EED in the propagation of repressive histone marks. *Nature* **461**, 762-767.
**Mellor, J.** (2006). It takes a PHD to read the histone code. *Cell* **126**, 22-24.
**Mikkelsen, T. S., Ku, M., Jaffe, D. B., Issac, B., Lieberman, E., Giannoukos, G., Alvarez, P., Brockman, W., Kim, T. K., Koche, R. P. et al.** (2007). Genome-wide maps of chromatin state in pluripotent and lineage-committed cells. *Nature* **448**, 553-560.
**Muller, J., Hart, C. M., Francis, N. J., Vargas, M. L., Sengupta, A., Wild, B., Miller, E. L., O'Connor, M. B., Kingston, R. E. and Simon, J. A.** (2002). Histone methyltransferase activity of a Drosophila Polycomb group repressor complex. *Cell* **111**, 197-208.
**Nagano, T., Mitchell, J. A., Sanz, L. A., Pauler, F. M., Ferguson-Smith, A. C., Feil, R. and Fraser, P.** (2008). The Air noncoding RNA epigenetically silences transcription by targeting G9a to chromatin. *Science* **322**, 1717-1720.
**Nakagawa, T., Kajitani, T., Togo, S., Masuko, N., Ohdan, H., Hishikawa, Y., Koji, T., Matsuyama, T., Ikura, T., Muramatsu, M. et al.** (2008). Deubiquitylation of histone H2A activates transcriptional initiation via trans-histone cross-talk with H3K4 di- and trimethylation. *Genes Dev.* **22**, 37-49.
**Navarro, P., Chambers, I., Karwacki-Neisius, V., Chureau, C., Morey, C., Rougeulle, C. and Avner, P.** (2008). Molecular coupling of Xist regulation and pluripotency. *Science* **321**, 1693-1695.
**Nekrasov, M., Wild, B. and Muller, J.** (2005). Nucleosome binding and histone methyltransferase activity of Drosophila PRC2. *EMBO Rep.* **6**, 348-353.
**Nekrasov, M., Klymenko, T., Fraterman, S., Papp, B., Oktaba, K., Kocher, T., Cohen, A., Stunnenberg, H. G., Wilm, M. and Muller, J.** (2007). Pcl-PRC2 is needed to generate high levels of H3-K27 trimethylation at Polycomb target genes. *EMBO J.* **26**, 4078-4088.
**O'Connell, S., Wang, L., Robert, S., Jones, C. A., Saint, R. and Jones, R. S.** (2001). Polycomblike PHD fingers mediate conserved interaction with enhancer of zeste protein. *J. Biol. Chem.* **276**, 43065-43073.
**Okamoto, I., Otte, A. P., Allis, C. D., Reinberg, D. and Heard, E.** (2004). Epigenetic dynamics of imprinted X inactivation during early mouse development. *Science* **303**, 644-649.
**Papp, B. and Muller, J.** (2006). Histone trimethylation and the maintenance of transcriptional ON and OFF states by trxG and PcG proteins. *Genes Dev.* **20**, 2041-2054.
**Pasini, D., Bracken, A. P., Hansen, J. B., Capillo, M. and Helin, K.** (2007). The polycomb group protein Suz12 is required for embryonic stem cell differentiation. *Mol. Cell. Biol.* **27**, 3769-3779.
**Pasini, D., Cloos, P. A., Walfridsson, J., Olsson, L., Bukowski, J. P., Johansen, J. V., Bak, M., Tommerup, N., Rappsilber, J. and Helin, K.** (2010). JARID2 regulates binding of the Polycomb repressive complex 2 to target genes in ES cells. *Nature* **464**, 306-310.
**Peng, J. C., Valouev, A., Swigut, T., Zhang, J., Zhao, Y., Sidow, A. and Wysocka, J.** (2009). Jarid2/Jumonji coordinates control of PRC2 enzymatic activity and target gene occupancy in pluripotent cells. *Cell* **139**, 1290-1302.
**Penny, G. D., Kay, G. F., Sheardown, S. A., Rastan, S. and Brockdorff, N.** (1996). Requirement for Xist in X chromosome inactivation. *Nature* **379**, 131-137.
**Plath, K., Fang, J., Mlynarczyk-Evans, S. K., Cao, R., Worringer, K. A., Wang, H., de la Cruz, C. C., Otte, A. P., Panning, B. and Zhang, Y.** (2003). Role of histone H3 lysine 27 methylation in X inactivation. *Science* **300**, 131-135.
**Plath, K., Talbot, D., Hamer, K. M., Otte, A. P., Yang, T. P., Jaenisch, R. and Panning, B.** (2004). Developmentally regulated alterations in Polycomb repressive complex 1 proteins on the inactive X chromosome. *J. Cell Biol.* **167**, 1025-1035.
**Sarma, K., Margueron, R., Ivanov, A., Pirrotta, V. and Reinberg, D.** (2008). Ezh2 requires PHF1 to efficiently catalyze H3 lysine 27 trimethylation in vivo. *Mol. Cell. Biol.* **28**, 2718-2731.
**Schuettengruber, B. and Cavalli, G.** (2009). Recruitment of polycomb group complexes and their role in the dynamic regulation of cell fate choice. *Development* **136**, 3531-3542.
**Sewalt, R. G., van der Vlag, J., Gunster, M. J., Hamer, K. M., den Blaauwen, J. L., Satijn, D. P., Hendrix, T., van Driel, R. and Otte, A. P.** (1998). Characterization of interactions between the mammalian polycomb-group proteins Enx1/EZH2 and EED suggests the existence of different mammalian polycomb-group protein complexes. *Mol. Cell. Biol.* **18**, 3586-3595.
**Sheardown, S. A., Duthie, S. M., Johnston, C. M., Newall, A. E., Formstone, E. J., Arkell, R. M., Nesterova, T. B., Alghisi, G. C., Rastan, S. and Brockdorff, N.** (1997). Stabilization of Xist RNA mediates initiation of X chromosome inactivation. *Cell* **91**, 99-107.
**Shen, X., Kim, W., Fujiwara, Y., Simon, M. D., Liu, Y., Mysliwiec, M. R., Yuan, G. C., Lee, Y. and Orkin, S. H.** (2009). Jumonji modulates polycomb activity and self-renewal versus differentiation of stem cells. *Cell* **139**, 1303-1314.
**Silva, J., Mak, W., Zvetkova, I., Appanah, R., Nesterova, T. B., Webster, Z., Peters, A. H., Jenuwein, T., Otte, A. P. and Brockdorff, N.** (2003). Establishment of histone h3 methylation on the inactive X chromosome requires transient recruitment of Eed-Enx1 polycomb group complexes. *Dev. Cell* **4**, 481-495.
**Simon, J., Chiang, A., Bender, W., Shimell, M. J. and O'Connor, M.** (1993). Elements of the Drosophila bithorax complex that mediate repression by Polycomb group products. *Dev. Biol.* **158**, 131-144.
**Simon, J. A. and Kingston, R. E.** (2009). Mechanisms of polycomb gene silencing: knowns and unknowns. *Nat. Rev. Mol. Cell Biol.* **10**, 697-708.
**Sing, A., Pannell, D., Karaiskakis, A., Sturgeon, K., Djabali, M., Ellis, J., Lipshitz, H. D. and Cordes, S. P.** (2009). A vertebrate Polycomb response element governs segmentation of the posterior hindbrain. *Cell* **138**, 885-897.
**Sparmann, A. and van Lohuizen, M.** (2006). Polycomb silencers control cell fate, development and cancer. *Nat. Rev. Cancer* **6**, 846-856.
**Stock, J. K., Giadrossi, S., Casanova, M., Brookes, E., Vidal, M., Koseki, H., Brockdorff, N., Fisher, A. G. and Pombo, A.** (2007). Ring1-mediated ubiquitination of H2A restrains poised RNA polymerase II at bivalent genes in mouse ES cells. *Nat. Cell Biol.* **9**, 1428-1435.
**Tie, F., Prasad-Sinha, J., Birve, A., Rasmuson-Lestander, A. and Harte, P. J.** (2003). A 1-megadalton ESC/E(Z) complex from Drosophila that contains polycomblike and RPD3. *Mol. Cell. Biol.* **23**, 3352-3362.
**Tie, F., Siebold, A. P. and Harte, P. J.** (2005). The N-terminus of Drosophila ESC mediates its phosphorylation and dimerization. *Biochem. Biophys. Res. Commun.* **332**, 622-632.
**Umlauf, D., Goto, Y., Cao, R., Cerqueira, F., Wagschal, A., Zhang, Y. and Feil, R.** (2004). Imprinting along the Kcnq1 domain on mouse chromosome 7 involves repressive histone methylation and recruitment of Polycomb group complexes. *Nat. Genet.* **36**, 1296-1300.
**Ura, H., Usuda, M., Kinoshita, K., Sun, C., Mori, K., Akagi, T., Matsuda, T., Koide, H. and Yokota, T.** (2008). STAT3 and Oct-3/4 control histone modification through induction of Eed in embryonic stem cells. *J. Biol. Chem.* **283**, 9713-9723.
**van den Berg, D. L., Zhang, W., Yates, A., Engelen, E., Takacs, K., Bezstarosti, K., Demmers, J., Chambers, I. and Poot, R. A.** (2008). Estrogen-

related receptor beta interacts with Oct4 to positively regulate Nanog gene expression. *Mol. Cell. Biol.* **28**, 5986-5995.
**van den Berg, D. L., Snoek, T., Mullin, N. P., Yates, A., Bezstarosti, K., Demmers, J., Chambers, I. and Poot, R. A.** (2010). An Oct4-centered protein interaction network in embryonic stem cells. *Cell Stem Cell* **6**, 369-381.
**Walker, E., Ohishi, M., Davey, R. E., Zhang, W., Cassar, P. A., Tanaka, T. S., Der, S. D., Morris, Q., Hughes, T. R., Zandstra, P. W. et al.** (2007). Prediction and testing of novel transcriptional networks regulating embryonic stem cell self-renewal and commitment. *Cell Stem Cell* **1**, 71-86.
**Walker, E., Chang, W. Y., Hunkapiller, J., Cagney, G., Garcha, K., Torchia, J., Krogan, N. J., Reiter, J. F. and Stanford, W. L.** (2010). Polycomb-like 2 associates with PRC2 and regulates transcriptional networks during mouse embryonic stem cell self-renewal and differentiation. *Cell Stem Cell* **6**, 153-166.
**Wang, H., Wang, L., Erdjument-Bromage, H., Vidal, M., Tempst, P., Jones, R. S. and Zhang, Y.** (2004). Role of histone H2A ubiquitination in Polycomb silencing. *Nature* **431**, 873-878.
**Wang, S., Yu, X., Zhang, T., Zhang, X., Zhang, Z. and Chen, Y.** (2004). Chick Pcl2 regulates the left-right asymmetry by repressing Shh expression in Hensen's node. *Development* **131**, 4381-4391.
**Wang, S., He, F., Xiong, W., Gu, S., Liu, H., Zhang, T., Yu, X. and Chen, Y.** (2007). Polycomblike-2-deficient mice exhibit normal left-right asymmetry. *Dev. Dyn.* **236**, 853-861.

# A noncoding RNA regulates the neurogenin1 gene locus during mouse neocortical development

Masahiro Onoguchi[a], Yusuke Hirabayashi[a], Haruhiko Koseki[b], and Yukiko Gotoh[a,1]

[a]Institute of Molecular and Cellular Biosciences, University of Tokyo, Tokyo 113-0032, Japan; and [b]RIKEN Center for Allergy and Immunology, Kanagawa 230-0045, Japan

Edited by Michael Eldon Greenberg, Harvard Medical School, Boston, MA, and approved September 5, 2012 (received for review February 20, 2012)

**The proneural basic helix–loop–helix (bHLH) transcription factor neurogenin1 (Neurog1) plays a pivotal role in neuronal differentiation during mammalian development. The spatiotemporal control of the *Neurog1* gene expression is mediated by several specific enhancer elements, although how these elements regulate the *Neurog1* locus has remained largely unclear. Recently it has been shown that a large number of enhancer elements are transcribed, but the regulation and function of the resulting transcripts have been investigated for only several such elements. We now show that an enhancer element located 5.8–7.0 kb upstream of the mouse *Neurog1* locus is transcribed. The production of this transcript, designated *utNgn1*, is highly correlated with that of *Neurog1* mRNA during neuronal differentiation. Moreover, knockdown of *utNgn1* by a corresponding short interfering RNA inhibits the production of *Neurog1* mRNA in response to induction of neuronal differentiation. We also found that production of *utNgn1* is suppressed by polycomb group (PcG) proteins, which inhibit the expression of *Neurog1*. Our results thus suggest that a noncoding RNA transcribed from an enhancer element positively regulates transcription at the *Neurog1* locus.**

The mammalian central nervous system (CNS) is composed of a great variety of neurons and glial cells, all of which must be generated from multipotential neural precursor cells (NPCs) in the correct number and at specific times and locations during embryogenesis (1, 2). Proneural basic helix–loop–helix (bHLH) proteins play central roles in the specification of neuronal fate and the subsequent differentiation processes (3). Among these proteins, neurogenin1 (Neurog1) is a key regulator of neuronal fate specification in various regions of the neural tube, including those that give rise to the neocortex, midbrain, hindbrain, and dorsal and ventral spinal cord of the CNS, as well as in portions of the peripheral nervous system (4–7). In the developing mouse neocortex, ablation of *Neurog1* along with the related protein neurogenin2 (Neurog2) results in the loss of deep-layer neurons (8), and conversely, overexpression of *Neurog1* results in premature neuronal differentiation of NPCs at the expense of glial fate (9, 10). These observations suggest that expression of the *Neurog1* and *Neurog2* genes must be tightly controlled in a spatiotemporal manner during development to ensure the generation of specific subsets of neurons and establishment of the fine architecture of the CNS.

Spatiotemporal control of gene expression is generally mediated by regulatory elements including enhancers. Previous studies have revealed several enhancer elements that control expression of the *Neurog1* gene, including the lateral stripe element (LSE), the anterior neural plate element (ANPE), and the LATE; which were originally identified as tissue-specific enhancers in zebrafish and found to be conserved among various vertebrate genomes including the mouse genome (11–13). Deletion of the 4-kb mouse genomic region including LATE and ANPE significantly reduced overall expression of *Neurog1* in a transgenic reporter assay (14). Therefore, although this 4-kb region has been implicated in tissue-specific regulation, it might also contain an essential general enhancer or locus control region. It has remained elusive, however, how these regions regulate *Neurog1* expression and how their activity is regulated.

Several molecules have been implicated in the regulation of *Neurog1* expression during neocortical development. For instance, Wnt signaling induces expression of *Neurog1* via β-catenin and T cell specific transcription factor (TCF)/lymphoid enhancer binding factor (LEF) transcription factors in neocortical NPCs (15, 16). The homeodomain transcription factor Pax6, which contributes to neocortical regional identity, also positively regulates expression of *Neurog1* (12, 17). In contrast, Polycomb group (PcG) proteins suppress the *Neurog1* promoter during the gliogenic stage of neocortical development when the neurogenic potential of NPCs is restricted (18). Whether or how these molecules affect the enhancers of *Neurog1* has remained unclear.

Various mechanisms have been proposed for the regulation of a gene by a corresponding enhancer (19). Classically, enhancers are viewed as clusters of DNA elements that bind transcription factors, which in turn interact with the mediator complex or transcription factor IID to facilitate the recruitment of RNA polymerase II (as well as that of chromatin modifying enzymes) to the promoter region through "DNA looping" (20). However, recent studies have indicated that enhancer sequences are not simply binding sites for transcription factors and cofactors; rather, many of them are also transcribed to generate noncoding RNAs when the transcription of corresponding genes takes place (21–26). The functions of such enhancer-associated noncoding RNAs have only just begun to be elucidated, such as in the case of those derived from the Snail1 and HoxA gene loci (23–25).

In this study, we found that an enhancer region spanning from between LATE and ANPE to LATE is transcribed in mouse neocortical NPCs and that expression of this transcript (designated *utNgn1*) correlates well with that of *Neurog1* mRNA. Knockdown experiments revealed that *utNgn1* is necessary for the effective transcription of *Neurog1* in neocortical NPCs, suggesting that one of the enhancers of the *Neurog1* locus functions via generation of its transcript. Furthermore, the amount of *utNgn1* was found to be increased by Wnt signaling and to be down-regulated by PcG proteins. We noticed that the *utNgn1* locus in neocortical NPCs harbors histone H3 lysine 27 trimethylation (H3K27me3), a histone mark catalyzed by PcG proteins, as well as histone H3 lysine 4 trimethylation (H3K4me3) and histone H3 lysine 9 or 14 acetylation (H3K9/K14ac), marks of active transcription (27). Our results thus suggest that the enhancer of *Neurog1* regulates the expression of *Neurog1* via its transcript, and PcG proteins suppress a target gene not only directly by occupying promoter regions but also indirectly by occupying their enhancers.

## Results

**_utNgn1_ Is Transcribed from an Enhancer Region of the _Neurog1_ Locus.** A 4-kb region located 3.8–7.8 kb upstream of the transcription start site (TSS) of mouse *Neurog1* has been implicated in regulation of *Neurog1* expression in most expression domains of the mouse embryo (14), suggesting the existence of a general enhancer within this region. Given that this region contains a CpG island (CGI) between ANPE and LATE (Fig. 1*A*), we hypothesized that it might be transcriptionally active (28). We therefore first examined

Author contributions: M.O., Y.H., and Y.G. designed research; M.O. and Y.H. performed research; H.K. contributed new reagents/analytic tools; M.O., Y.H., and Y.G. analyzed data; and M.O., Y.H., and Y.G. wrote the paper.

The authors declare no conflict of interest.

This article is a PNAS Direct Submission.

[1]To whom correspondence should be addressed. E-mail: ygotoh@iam.u-tokyo.ac.jp.

This article contains supporting information online at www.pnas.org/lookup/suppl/doi:10.1073/pnas.1202956109/-/DCSupplemental.

whether the region surrounding this CGI contains the H3K4me3 mark, which is associated with the promoters of actively transcribed genes (or genes in a state permissive for transcription). We cultured NPCs prepared from the mouse neocortex at embryonic day (E) 11.5 for 3 d in vitro (DIV) as neurospheres (E11.5 + 3DIV culture). Chromatin immunoprecipitation (ChIP) assay revealed the presence of this modification in the region ~7 kb upstream of the TSS of *Neurog1* (Fig. 1*A*, primer 5), with a peak in H3K4me3 at the CGI (Fig. 1*B*). The amount of H3K4me3 at the CGI was similar to that at the promoter of *Neurog1* as well as at the promoter of the actively transcribed gene *Gapdh*, suggesting that the region surrounding the CGI might be transcribed. This notion was further supported by the observation that H3K9/K14ac, another histone modification associated with actively transcribed genes, was also present in the region surrounding the CGI (Fig. 1*C*).

We next performed RT-PCR analysis to search for transcripts derived from the region surrounding the CGI and detected PCR amplicons originating from a position ~6.1 kb upstream of the TSS of *Neurog1* in the mouse neocortex at E13.5 (Fig. 1 *A* and *D*). Furthermore, quantitative RT-PCR (qRT-PCR) analysis revealed that a significant level of transcription occurs in this position compared with other intergenic regions such as ~1.2, 3.6, and 4.6 kb upstream of the TSS of *Neurog1* (Fig. 1 *A* and *E*). Next, to determine the 5′ and 3′ ends of the transcripts, we performed rapid amplification of cDNA ends (RACE) analysis (Fig. 1*F*). 5′ RACE revealed multiple 5′ ends within the CGI, consistent with previous observations showing that CGI promoters are accompanied by multiple initiation points within the CGI (29). 3′ RACE revealed a polyadenylation signal at position −5.8 kb relative to the TSS of *Neurog1*. Consistent with these observations, Northern blot analysis with an antisense probe corresponding to positions −6.0 to −6.4 kb revealed a transcript of ~1.4 kb in a total RNA fraction isolated from the mouse neocortex at E13.5 (Fig. 1*G*). We now refer to this transcript derived from an enhancer region of *Neurog1* as *utNgn1* (upstream transcript of the *Neurog1* locus). The longest ORF of *utNgn1* potentially encodes a 49-amino-acid protein with

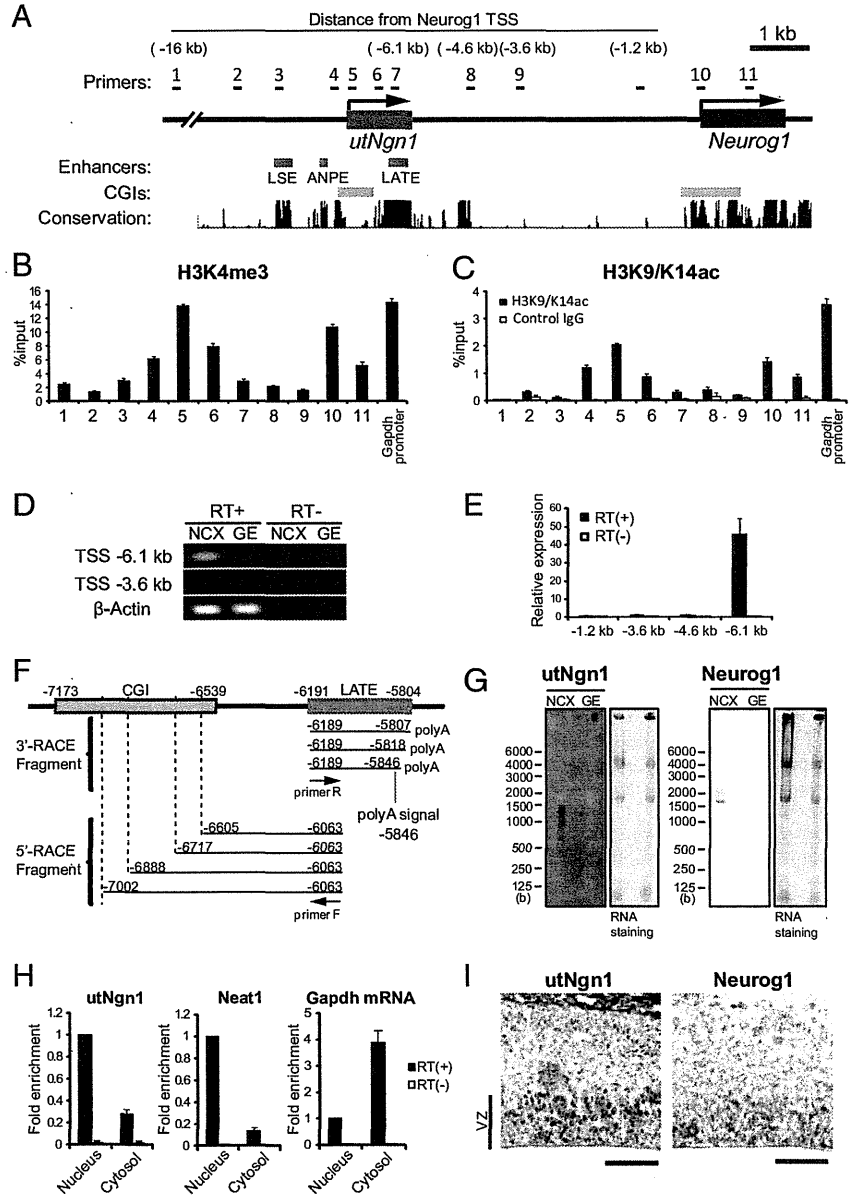


**Fig. 1.** A noncoding RNA, *utNgn1*, is transcribed from an enhancer region of *Neurog1*. (*A*) Schematic representation of enhancers and CpG islands (CGIs) of the mouse *Neurog1* locus. Blue and green boxes indicate enhancers (LATE, ANPE, and LSE) identified in zebrafish and CGIs, respectively. Black arrows indicate the direction of transcription of *utNgn1* (red box) and *Neurog1* (black box). Conservation plot and CGIs are adapted from the University of California Santa Cruz Genome Browser. Black bars indicate the positions of PCR primers used for RT-PCR or ChIP analysis. (*B* and *C*) Primary NPCs isolated from the E11.5 mouse neocortex (NCX) were cultured in suspension for 3DIV in the presence of fibroblast growth factor 2 (FGF2) and epidermal growth factor (EGF). Cells were then subjected to ChIP analysis with antibodies to H3K4me3 (*B*) or H3K9/K14ac (or with control IgG) (*C*) and with the PCR primers indicated in *A* or those specific for the promoter of *Gapdh*. Data are expressed as percentage of the input and are means ± SEM for three samples. (*D*) Total RNA extracted from the NCX or ganglionic eminences (GE) of E13.5 mouse embryos was subjected to RT (or not) with an oligo (dT) primer followed by PCR with primers targeted to regions located 6.1 kb or 3.6 kb upstream of the transcription start site (TSS) of *Neurog1* as well as with those specific for β-actin (internal control). (*E*) Relative expression levels of *utNgn1* locus (*Neurog1* TSS −6.1 kb) in the neocortex compared with other intergenic regions (*Neurog1* TSS −1.2, −3.6, and −4.6 kb) are determined by qRT-PCR. Data represent means ± SEM from three embryos at E13.5. (*F*) 5′ and 3′ RACE analysis of *utNgn1* with cDNA prepared from poly(A)$^+$ or total RNA of the mouse neocortex at E12.5. Black arrows indicate PCR primers F and R. Four 5′ ends and three 3′ ends were determined by DNA sequencing in 5′ RACE and 3′ RACE, respectively. Amplified fragments are mapped on the *Neurog1* upstream region, and a polyadenylation signal (AAATAA) is shown. (*G*) Northern blot analysis of total RNA prepared from the E13.5 NCX or GE were performed with DIG-labeled RNA probes specific for *utNgn1* or *Neurog1* mRNA. Blots were also stained with SYBR Gold (*Right*). (*H*) Relative concentration of *utNgn1* in the nuclear and cytosolic fractions. Cells were prepared from the E12.5 mouse NCX and cultured in suspension for 3DIV. The same amount of total RNA extracted from nuclear or cytosolic fractions of NPCs were reverse transcribed. Relative amounts of the cDNA in each fraction were determined by qRT-PCR. Data are expressed relative to the corresponding value for concentration in the nuclear fraction and are means ± SEM from three independent experiments. (*I*) In situ hybridization analysis of *utNgn1* and *Neurog1* mRNA in coronal sections of the E13.5 mouse NCX. VZ, ventricular zone. (Scale bar, 50 μm.)

no sequence similarity to any expressed sequences currently deposited in protein databases. Moreover, it may not be translated because fractionation of neocortical NPCs (E12.5 + 3DIV culture) revealed that the concentration of *utNgn1* is higher in the nucleus compared with the cytosol, which is characteristic of noncoding RNA (for instance, *Neat1*, *Malat1*, or *Xist*) (30) in contrast to the cytosol-enriched localization of coding RNA (mRNA) (Fig. 1*H*). We cannot, however, exclude the possibility that *utNgn1* is translated. Although *utNgn1* and *Neurog1* mRNA are encoded on the same strand, they do not appear to be components of the same transcript, given that neither the probe for *utNgn1* nor one for *Neurog1* mRNA detected a transcript spanning both target RNAs (>3 kb) in Northern blot analysis (Fig. 1*G*). In addition, we could not detect a transcript, by qRT-PCR, or association with histone H3 lysine 36 trimethylation (H3K36me3) (27), by ChIP analysis, for the region between the coding sequences for *utNgn1* and *Neurog1* mRNA (Fig. 1*E* and Fig. S1).

**Correlation Between *utNgn1* and *Neurog1* mRNA Expression Patterns.** Long noncoding RNAs have previously been found to affect gene expression both positively and negatively (31). We therefore compared the expression pattern of *utNgn1* with that of *Neurog1* mRNA. We isolated various regions of the developing CNS, including the neocortex, ganglionic eminences, diencephalon, midbrain, hindbrain, and spinal cord, as well as nonneural tissues, including the heart, liver, and limb, from mouse embryos at E13.5. qRT-PCR analysis revealed that *utNgn1* was expressed in all regions of the CNS that expressed *Neurog1* mRNA, but neither RNA was detected in the nonneural tissues (Fig. 2*A*) (14). Moreover, the amount of *utNgn1* correlated well with that of *Neurog1* mRNA. The expression level of *utNgn1* is very low (1/30–1/300 of that of *Neurog1*) (Fig. 2 *A–D*). Northern blot analysis also showed that both *utNgn1* and *Neurog1* mRNA were more abundant in the neocortex than in the ganglionic eminences (Fig. 1*G*). These results thus suggested that the expression of *utNgn1* is positively correlated with that of *Neurog1* mRNA.

We also examined the expression of *utNgn1* by in situ hybridization. An antisense probe for *utNgn1* yielded robust signals in a subpopulation of cells located within the ventricular zone (which contains NPCs) of the E13.5 mouse neocortex (Fig. 1*I*), the midbrain, and a dorsal part of the diencephalon (Fig. S2 *A* and *B*). Importantly, the expression pattern of *utNgn1* largely overlapped with that of *Neurog1* mRNA, providing further support for a positive correlation between *utNgn1* and *Neurog1* mRNA expression in the developing CNS.

We next asked whether the expression level of *utNgn1* changes during neuronal differentiation of neocortical NPCs. NPCs freshly prepared from the neocortex at E11.5 were maintained in an undifferentiated state in the presence of fibroblast growth factor (FGF)2. Removal of FGF2 in such primary cultures results in neuronal differentiation and promotes the production of *Neurog1* mRNA and subsequently that of *βIII-tubulin* mRNA (32) (Fig. 2*B*). Here we found that, under the same conditions, growth factor deprivation also induced expression of *utNgn1* with a time course similar to that of *Neurog1* mRNA (Fig. 2*B*), indicating that the expression of *utNgn1* positively correlates with that of *Neurog1* mRNA and is induced during an early phase of neuronal differentiation of neocortical NPCs.

We next investigated how the production of *utNgn1* is regulated by extracellular signals, which regulate neuronal differentiation of NPCs. Notch signaling is essential for the maintenance of undifferentiated state of NPCs and suppress neuronal differentiation. We then induced neuronal differentiation of NPCs by treatment with *N*-[*N*-(3,5-difluoro-phenacetyl)-L-alanyl]-(*S*)-phenylglycine *t*-butyl ester (DAPT), a presenilin inhibitor that suppresses Notch signaling and thereby reduces the amount of *Hes1* and *Hes5* mRNA, a downstream effector of Notch signaling (33) (Fig. 2*C*). Exposure of the NPC cultures to DAPT induced the expression of *utNgn1* and that of *Neurog1* mRNA (Fig. 2*C*). Wnt signaling is another extracellular signaling that regulates neuronal differentiation and *Neurog1* expression in the mouse neocortex. We therefore examined whether Wnt signaling might also regulate *utNgn1* expression. Treatment of E11.5 neocortical NPCs with recombinant Wnt3a for 9 or 24 h increased the amounts of *utNgn1* and of *Neurog1* mRNA (Fig. 2*D*). These results further indicate that the expression of *utNgn1* positively correlates with that of *Neurog1* mRNA and is induced during neuronal differentiation of neocortical NPCs.

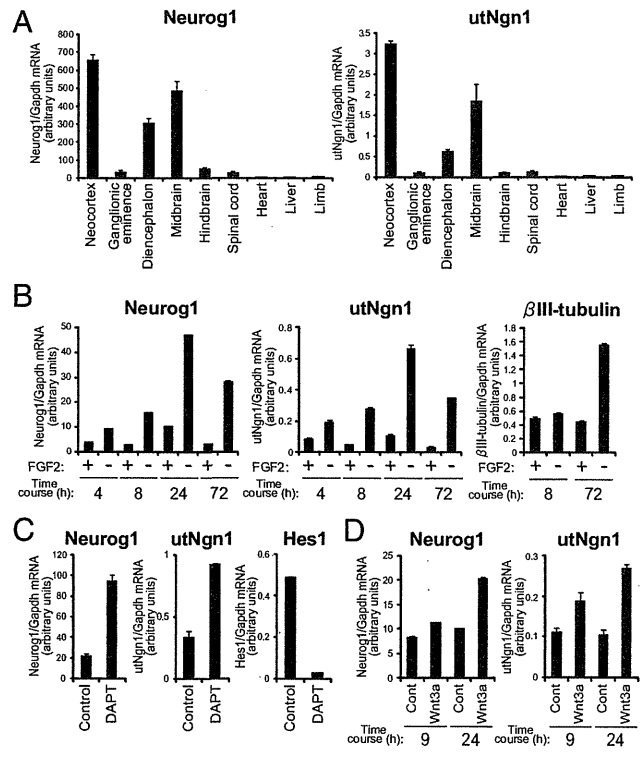


**Fig. 2.** Expression pattern of *utNgn1* is highly correlated with that of *Neurog1* mRNA. (*A*) Tissues were isolated from the neocortex, ganglionic eminences, diencephalon, midbrain, hindbrain, spinal cord, heart, liver, and limb of E13.5 mouse embryos. (*B*) Primary NPCs prepared from the E11.5 neocortex were cultured for 1 d and then incubated for the indicated times in medium with or without FGF2. (*C*) Primary NPCs prepared from the E11.5 neocortex were cultured for 2 d and then exposed to DAPT (5 μM) or dimethyl sulfoxide vehicle (control) for 7 h. (*D*) Primary NPCs prepared from the E11.5 neocortex were cultured without (control) or with Wnt3a for 9 or 24 h. (*A–D*) Total RNA was isolated from the cells or tissues and subjected to qRT-PCR analysis of each gene. Relative amounts of *Neurog1* and *utNgn1* were determined using a standard curve derived from a BAC clone, which contained both *Neurog1* and *utNgn1* loci, making the values of *Neurog1* and *utNgn1* transcripts comparable. Data are normalized by the amount of *Gapdh* mRNA and are means ± SEM ($n = 3$).

We also examined the expression of *utNgn1* in embryonic stem (ES) cells and ES-derived NPCs (Fig. S3) (34). Neither *utNgn1* nor *Neurog1* mRNA was detected in ES cells in the undifferentiated state (day 0), but both transcripts were found to be expressed after culturing the cells for 7 d under conditions that induce differentiation into NPCs (day 7). Again, these results supported a positive correlation between transcription of *utNgn1* and that of *Neurog1* mRNA during development.

***utNgn1* Positively Regulates *Neurog1* Expression.** Transcription of neighboring loci can be positively correlated as a result of the phenomenon known as transcriptional noise or "ripples" (35), which might be dependent on mechanisms including chromatin remodeling. We therefore investigated whether *utNgn1* functions in gene regulation or is simply a byproduct of *Neurog1* expression. To assess its possible role in *Neurog1* expression, we knocked down *utNgn1* in E11.5 NPCs using small interfering RNAs (siRNAs) targeted to three different sequences within *utNgn1* and three control siRNAs. Growth factor deprivation for 10 h induced *Neurog1* expression in cells without siRNA or with control siRNA, but this effect was markedly inhibited in cells harboring any of the

DEVELOPMENTAL BIOLOGY

siRNAs specific for *utNgn1* (Fig. 3*A* and Fig. S4). We confirmed that the nuclear level of *utNgn1* was effectively decreased by siRNAs targeting *utNgn1* (Fig. 3*B*). We examined the expression of genes within 1 Mb of the *utNgn1* locus and found that knockdown of *utNgn1* did not reduce the expression of any of these genes except for *Neurog1* (Fig. 3*C* and Fig. S5 *A* and *B*). We also found that depletion of *Neurog1* mRNA with a corresponding siRNA did not affect the amount of *utNgn1* (Fig. 3*D*). These results thus suggest that *utNgn1* is not simply a byproduct of transcription of a neighboring gene, but rather is a positive regulator of *Neurog1* expression, providing an example of gene regulation through the production of an enhancer-derived transcript.

Next we examined the biological function of *utNgn1*. Consistent with the proposed role of *Neurog1* in neuronal fate commitment in neocortical NPCs (8), we found that *utNgn1* knockdown partially inhibited the induction of *Tbr2* and *NeuroD1*, early markers of neocortical neuronal fate commitment, under a differentiation-inducing condition (Fig. S5*C*). Therefore, *utNgn1* might play a role in neuronal fate commitment of these cells.

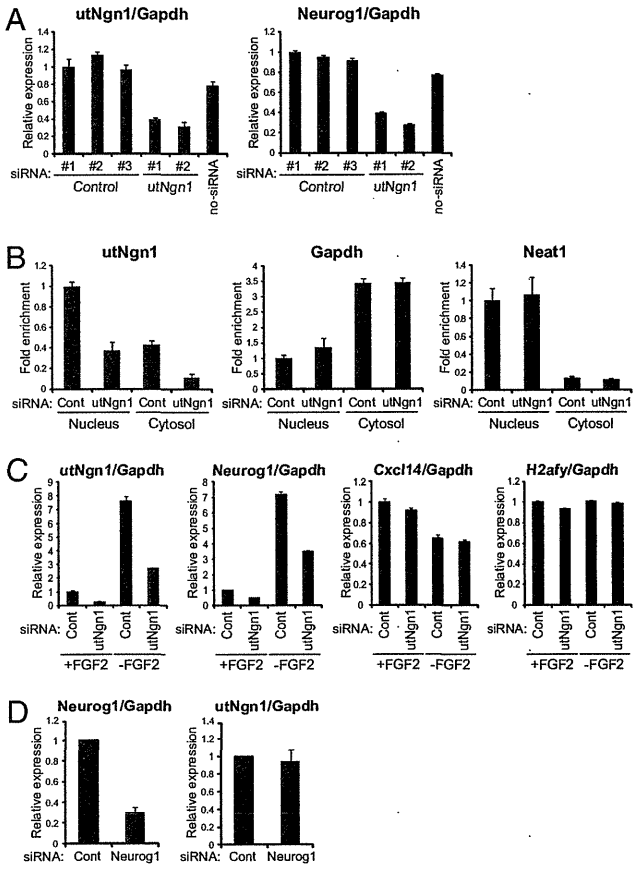


**Fig. 3.** *utNgn1* is required for the expression of *Neurog1* during neuronal differentiation. (*A*, *C*, and *D*) Primary NPCs prepared from the E11.5 neocortex were transfected with three independent control (siRNAs 1, 2, and 3), two independent siRNAs against *utNgn1* (*utNgn1* siRNA 1 and 2), or without siRNAs (no-siRNA) (*A*). Similarly, cells were transfected with control (siRNA 1), *utNgn1* (siRNA 1), or siRNA against *Neurog1* (*C* and *D*). Cells were cultured for 2 d with FGF2 and then for 10 h with or without FGF2. Total RNA was then extracted from the cells and subjected to qRT-PCR analysis of each gene. Data are normalized with the amount of *Gapdh* mRNA, are expressed relative to the corresponding value for cells transfected with the control siRNA 1, and are means ± SEM ($n = 3$). (*B*) Primary NPCs prepared from the E11.5 neocortex were transfected with a control (siRNA 1) or with a combination of two independent siRNAs against *utNgn1* (*utNgn1* siRNAs 1 and 2). Cells were cultured for 3 d in suspension with FGF2 and EGF, harvested and fractionated, as described in Fig. 1*H*, and the amount of RNA in each fraction was determined.

***utNgn1*, but Not Its Truncated Form, Positively Regulates Expression of Its Downstream Gene.** To investigate whether *utNgn1* is capable of *cis*-regulating the transcription of its downstream gene, we performed a reporter gene assay. We designed Firefly luciferase (luc2) reporter constructs as schematized in Fig. 4*A*. In these constructs, the luc2 gene is under the control of the *Neurog1* promoter either alone (*a*), with an intact *utNgn1* (*b*), or with a truncated *utNgn1* harboring early termination sequences (*c*). In vector *c*, we inserted early termination sequences in *utNgn1* between the CGI and the LATE enhancer to inhibit the expression of full-length *utNgn1* without affecting the LATE enhancer sequence itself. A synthetic poly(A) signal transcriptional pause site was inserted between *utNgn1* and the *Neurog1* promoter to prevent the direct effect of upstream transcription on reporter transcription. We found that the insertion of *utNgn1* into an upstream region of the *Neurog1* promoter significantly enhanced reporter gene transcription (Fig. 4*B*). Importantly, insertion of early termination sequences in *utNgn1* resulted in a loss of the increased reporter gene expression, suggesting the importance of an intact *utNgn1* transcript for this action (Fig. 4*B*). This result provides additional evidence indicating the importance of *utNgn1* for *Neurog1* gene transcription.

**PcG Proteins Suppress *utNgn1* Expression.** During the late stage of neocortical development, which is associated with the restriction of neuronal fate and activation of the gliogenic phase of NPCs, PcG proteins suppress the *Neurog1* promoter (18). We therefore asked whether PcG proteins also regulate *utNgn1* expression. ChIP analysis with neocortical NPCs (E11.5 + 3DIV or 9DIV) revealed that the *utNgn1* locus was broadly occupied by H3K27me3, a histone mark catalyzed by PcG proteins, at levels comparable to those at the promoter of *Neurog1* (Fig. 5*A*). Therefore, like the *Neurog1* locus, the *utNgn1* locus is also "bivalent," harboring both H3K4me3 (active) and H3K27me3 (repressive) histone marks (36). Neocortical E11.5 + 3DIV and E11.5 + 9DIV NPC cultures are characterized by preferential differentiation into neurons and astrocytes, respectively, under the conditions adopted in the present study (18). The level of H3K27me3 at the *utNgn1* locus was substantially higher in E11.5 + 9DIV cultures than in E11.5 + 3DIV cultures (Fig. 5*A*), suggesting that this change is associated with the late (gliogenic) stage of neocortical NPC development. In contrast, the level of H3K4me3 at both *utNgn1* and *Neurog1* loci remained largely unchanged between E11.5 + 3DIV and E11.5 + 9DIV (Fig. 5*B*).

The high levels of H3K27me3 at the *utNgn1* locus suggest that PcG proteins may suppress the production of the enhancer-encoded transcript during the late developmental stage of neocortical NPCs. To test this hypothesis, we first examined whether the expression of *utNgn1* is indeed repressed in the late stage of neocortical NPC development. The level of *utNgn1*, as well as that of *Neurog1* mRNA, was greatly reduced in E11.5 + 9DIV cultures compared with that in E11.5 + 3DIV cultures (Fig. 5*C*). We observed similar reductions of both *utNgn1* and *Neurog1* in E17.5 + 3DIV cultures relative to E11.5 + 3DIV cultures (Fig. 5*C*), suggesting that the suppression of *utNgn1* expression is the result of developmental progression rather than culture duration. Consistent with this, the expression levels of both *Neurog1* and *utNgn1* in the neocortex were dramatically reduced during development (Figs. S2*C* and S6). We then examined whether the suppression of *utNgn1* production in the late stage of development is mediated by PcG proteins. To this end, we induced the conditional ablation of Ring1B, an essential component of Polycomb repressive complex 1 (37), by injecting tamoxifen intraperitoneally into *Ring1b*$^{flox/flox}$; NestinERT2-Cre mice (18, 38) at E12.5. The amount of *utNgn1* was markedly greater in the neocortex isolated from the Ring1B-deficient embryos at E18.5 compared with control embryos (Fig. 5*D*). Together, these results indicate that PcG proteins suppress *utNgn1* expression during the late stage of neocortical NPC development. PcG proteins thus appear to regulate *Neurog1* expression not simply by direct suppression of the gene itself but also by that of its enhancer.

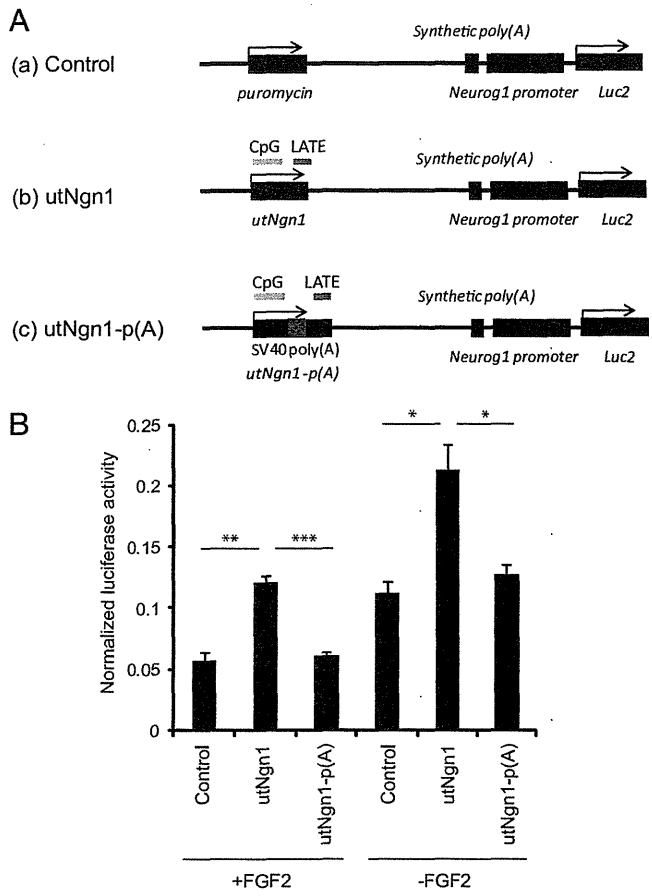


**Fig. 4.** Full-length *utNgn1*, but not truncated *utNgn1*, promotes expression of reporter gene. (*A*) Schematic representation of the reporter constructs. A 2.7-kb region of the Neurog1 promoter was cloned into the promoter multicloning site of the pGL4.20 vector and used as a control (*a*). Full-length *utNgn1* was cloned and inserted into the upstream region of vector *a* (*b*). Two SV40 poly(A) sequences were tandemly inserted into the *utNgn1* region between the CGI and the LATE enhancer (*c*). (*B*) Luciferase reporter assay. Firefly vectors shown in *A* and the control Renilla vector were transfected into NPCs prepared from E11.5 neocortices. All cells were cultured with FGF2 for 12 h and then half were cultured with and half without FGF2 for 20 h. Data are normalized by the Renilla luciferase activity and are means ± SEM ($n = 3$). $^*P < 0.05$, $^{**}P < 0.01$, $^{***}P < 0.001$ by two-tailed Student *t* test.

## Discussion

A significant portion of the mammalian genome generates noncoding RNAs (ncRNAs) including long intervening noncoding RNAs (lincRNAs) (39–41), some of which have been implicated in gene silencing associated with processes such as imprinting and X chromosome inactivation (42). However, recent studies have also begun to reveal roles of lincRNAs in gene activation (23–25). For instance, a set of ncRNAs (ncRNA-a) was shown to positively regulate their neighboring protein-coding genes, including those for *SCL*, *Snail1*, and *Snail2* (24). Similarly, *HOTTIP*, a lincRNA transcribed from the 5′ end of the *HoxA* locus, was found to positively regulate the *HoxA* gene cluster (23). Our results now indicate that *utNgn1* is another lincRNA that positively regulates gene expression.

Recent genome-wide studies have revealed that gene promoters are marked by H3K4me3, whereas enhancers are often associated with H3K4me1 but are devoid of H3K4me3 (43). The enhancer region now shown to encode *utNgn1* therefore appears to be atypical in that it is associated with H3K4me3. Because this is also the case for the ncRNA-a and *HOTTIP* loci, the presence of H3K4me3 in the enhancer regions might be a specific characteristic of regions encoding this "gene activator" class of lincRNAs. H3K4me1-enriched enhancers have also been shown to express RNA (eRNA), although the functions of these RNA molecules are unknown (21, 26). The transcripts from H3K4me1-enriched enhancers are devoid of polyadenylation, whereas long noncoding RNAs transcribed from H3K4me3-enriched enhancers including *utNgn1* harbor polyadenylation, possibly reflecting a difference in mode of regulation and/or function (21, 23–26). *utNgn1* is more similar to lincRNAs in this context, although the *utNgn1* locus does not harbor the H3K36me3 mark, which is a characteristic of lincRNAs.

Development is associated with strict regulation of the enhancers of developmental genes. It has been proposed that H3K4me1-enriched enhancers can be classified as either "poised" and "active" enhancers by the additional presence of the histone marks H3K27me3 and H3K27ac, respectively (44, 45). It remains unclear, however, whether these histone marks are functionally important for enhancer activity. Our results now suggest that the

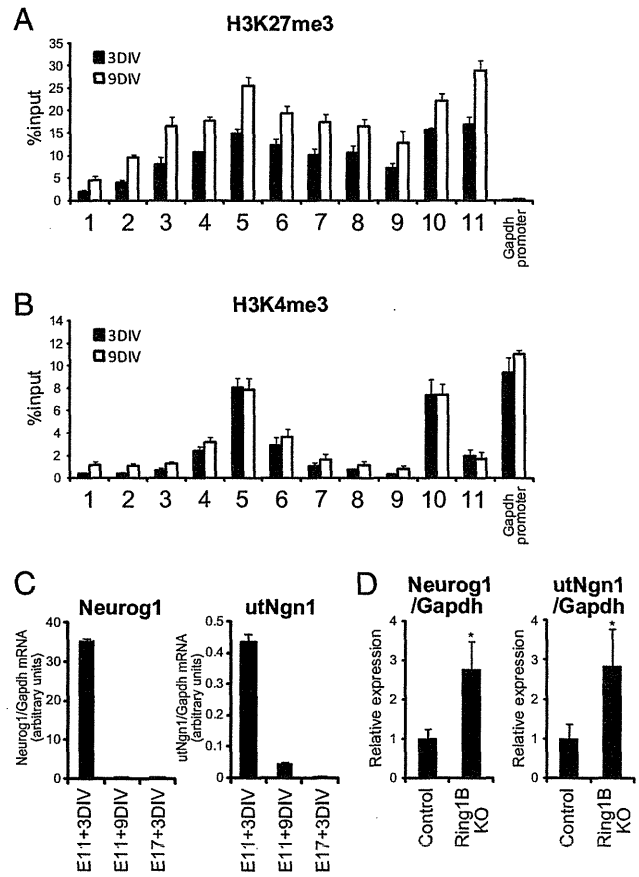


**Fig. 5.** PcG proteins repress the expression of *utNgn1* in the late stage of NPC development. (*A* and *B*) Primary NPCs isolated from the E11.5 neocortex were cultured for 3 or 9 DIV in suspension in the presence of FGF2 and EGF. Cells were then subjected to ChIP assays with antibodies to H3K27me3 (*A*) or to H3K4me3 (*B*) and with the PCR primers indicated in Fig. 1*A*. Data are means ± SEM from three independent experiments. (*C*) Primary NPCs isolated from the E11.5 or E17.5 neocortex were cultured for 3 or 9 DIV as in *A*, after which total RNA was isolated and subjected to qRT-PCR analysis of *utNgn1* and *Neurog1* mRNA. Data are normalized by the amount of *Gapdh* mRNA and are means ± SEM ($n = 3$). (*D*) Total RNA prepared from the neocortex of E18.5 *Ring1b*$^{flox/flox}$; NestinERT2-Cre (Ring1B KO) and *Ring1-b*$^{flox/flox}$ (control) embryos that were exposed to tamoxifen in utero at E12.5 were subjected to qRT-PCR analysis of *Neurog1* mRNA and *utNgn1*. Data are normalized by the amount of *Gapdh* mRNA, are expressed relative to the corresponding value for control embryos, and are means ± SD from three embryos of each genotype. $^*P < 0.05$ (Student *t* test).